The emergence and evolution of Santa Maria Island (Azores) – the conundrum of uplifted islands revisited

Ricardo S. Ramalho[1,2], George Helffrich[3], José Madeira[4,5], Michael Cosca[6], Christine Thomas[7], Rui Quartau[8,5], Ana Hipólito[9], Alessio Rovere[10], Paul J. Hearty[11], and Sérgio P. Ávila[12,13]

[1] *School of Earth Sciences, University of Bristol, Wills Memorial Building, Queen's Road, Bristol, BS8 1RJ, UK.*

[2] *Lamont-Doherty Earth Observatory at Columbia University, Comer Geochemistry Building, 61 Route 9W/ PO box 1000, Palisades, NY-10964-8000, USA.*

[3] *Earth-Life Science Institute, Tokyo Institute of Technology, 2-12-1-IE-1 Ookayama, Meguro-ku, Tokyo, 152-8550, Japan*

[4] *Departamento de Geologia, Faculdade de Ciências, Universidade de Lisboa, 1749-016, Lisboa, Portugal.*

[5] *Instituto Dom Luiz, Faculdade de Ciências, Universidade de Lisboa, 1749-016, Lisboa, Portugal.*

[6] *U.S. Geological Survey, Denver Federal Center, MS 963, Denver, CO 80225, USA.*

[7] *Institut für Geophysik, Westfälische Wilhelms-Universität, Correnssstraße 24, 48149 Münster, Germany*

[8] *Divisão de Geologia Marinha, Instituto Hidrográfico, Rua das Trinas, 49, 1249-093 Lisboa, Portugal*

[9] *Instituto de Investigação em Vulcanologia e Avaliação de Riscos, Universidade dos Açores, Rua da Mãe de Deus, Edifício do Complexo Científico, 3º Andar - Ala Sul, 9500-321 Ponta Delgada, Açores, Portugal.*

[10] *MARUM, University of Bremen and ZMT, Leibniz Center for Tropical Marine Ecology, Marum Pavillion 1110, Bremen, Germany*

[11] *Department of Environmental Studies, University of North Carolina Wilmington, NC-28403, USA*

[12] *Faculdade de Ciências da Universidade do Porto, Rua do Campo Alegre s/n, 4169-007 Porto, Portugal.*

[13] *CIBIO, Centro de Investigação em Biodiversidade e Recursos Genéticos, InBIO Laboratório Associado, Pólo dos Açores, Departamento de Biologia da Universidade dos Açores, Campus de Ponta Delgada, Apartado 1422, 9501-801 Ponta Delgada, Açores, Portugal*

ABSTRACT

The growth and decay of ocean island volcanoes is intrinsically linked to vertical movements; whilst the causes for subsidence are well understood, uplift mechanisms remain enigmatic. Santa Maria Island in the Azores Archipelago is an ocean island volcano resting on top of young lithosphere, barely 480 km away from the Mid-Atlantic Ridge. Like most other Azorean islands, Santa Maria should be experiencing subsidence. Yet, several features indicate an uplift trend instead. In this paper we reconstruct the evolutionary history of Santa Maria with respect to the timing and magnitude of its vertical movements, using detailed fieldwork and $^{40}Ar/^{39}Ar$ geochronology. Our investigations revealed a complex evolutionary history spanning ~6 Ma, with subsidence followed by uplift extending to the present day. The fact that an island

located in young lithosphere experienced such a pronounced uplift trend is remarkable and raises important questions concerning possible uplift mechanisms. Localized uplift in response to the tectonic regime affecting the southeastern tip of the Azores Plateau is unlikely since the area is under transtension. Our analysis shows that the only viable mechanism able to explain the uplift is crustal thickening by basal intrusions, suggesting that intrusive processes play a significant role even on islands standing on young lithosphere, such as in the Azores.

INTRODUCTION

Ocean island volcanoes are typically subjected to long-term subsidence, as the linear, age-progressive island chains of the Pacific Ocean clearly exemplify. This subsidence trend is essentially driven by mechanisms such as volcanic surface loading (Moore, 1970; Walcott, 1970; Menard, 1983), plate cooling with age (Parsons and Sclater, 1977; Stein and Stein, 1992), and hotspot swell decay (Morgan et al., 1995), all of which are influenced by fast plate movement away from the melting source. All these mechanisms (with perhaps the exception of hotspot swell decay) are reasonably well understood and are consistent within the plate tectonics/isostasy framework. In a similar fashion, within this fast-moving plate scenario, uplift episodes are easily explained by plate bending due to surface loading of younger islands further "upstream" along the chain (Walcott, 1970; Huppert et al., 2015), or by outer trench rise for islands approaching a subduction zone (Schmidt and Schmincke, 2000). A few island systems (e.g. the Cape Verdes, the Canaries, and Madeira Archipelago), however, fall out of pattern and feature numerous volcanic edifices that experienced pronounced uplift trends, vertical stability, or complex uplift/subsidence histories (e.g. Stautigel and Schmincke, 1984; Klügel et al., 1995; Schmidt and

Schmincke, 2002; Menendez et al., 2008; Ramalho et al., 2010a,b,c; Madeira et al., 2010; Sepúlveda et al., 2015; Ramalho et al., 2015). These are mostly concentrated in – but not restricted to – the NE Atlantic, where the Nubian plate moves very slowly or is quasi-stationary with respect to the islands' melting source (Burke and Wilson, 1972; Ramalho et al., 2010b; Ramalho et al., 2015). The mechanisms behind such uplift trends or episodes, however, are still not completely understood and are the subject of contemporaneous debate, being the focus of the present study.

Several plausible mechanisms have been put forward to explain ocean island uplift, all of which are likely to contribute in greater or lesser degree to the observed uplift trends/episodes. For uplift acting at broad regional scale, hotspot swell growth by either spreading of melt residue or dynamic topography is regarded as the most plausible mechanism (Morgan et al., 1995; Zhong and Watts, 2002; Ramalho et al., 2010b; Wilson et al., 2010, Ramalho, 2011). At smaller regional scales uplift may be generated by flexural uplift at the forebulge created by surface loading of nearby younger islands/seamounts (McNutt and Menard, 1978; Watts and ten Brink, 1989; Grigg and Jones, 1997; Huppert et al., 2015), by flexural uplift induced by subsurface loads ("underplating")(Watts and ten Brink, 1989; Ali et al., 2003), or by flexural rebound driven by mass wasting or erosion (Menard, 1983; Smith and Wessel, 2000; Menendez et al., 2008). However, these uplift mechanisms still act upon a wide area (which largely depends on plate rheology) and thus cannot be accounted to explain contrasting uplift histories for edifices spatially close together (Ramalho et al., 2010a,b,c). Additionally, surface loading has been shown to only generate uplift in the order of 10's of meters (unless unrealistically thin elastic thicknesses are considered)(McNutt and Menard, 1978). It also requires younger edifices being loaded at a suitable distance, and fails to explain long-term uplift trends. In a similar fashion, significant uplift by erosive flexural rebound is problematic because it requires large volumes of eroded/mass wasted material, or because the effects of redistribution of wasted materials over wider areas need to be accounted for (Smith and Wessel, 2000). At local (island) scale, possibly only repeated intrusions at crustal level are capable of explaining pronounced, long-term uplift trends and episodes, as it has been proposed for slow-moving or quasi-stationary hotspot settings such as the Cape Verde, Madeira, and Canary Archipelagos (Klügel et al., 2005; Ramalho et al., 2010a,b,c; Madeira et al., 2010; Ramalho et al., 2015; Klügel et al., 2015). However, in order to gain a better insight on the origins of pronounced, long-term ocean island uplift trends, further evidence is needed from different geodynamic settings, particularly from those where known uplift/subsidence models apply.

In this paper we further explore the enigmatic origins of ocean island uplift, using Santa Maria Island in the Azores Archipelago as a case study. Santa Maria is barely 480 km away from the Mid-Atlantic Ridge and consequently rests on young lithosphere. As such, like most of the other Azorean islands, the expectation for Santa Maria is that it should have been subjected to long-term subsidence. However it has long been recognized that this island must have experienced significant uplift due to the presence of raised shore platforms and the abundance of exposed marine volcanic and sedimentary sequences well above present sea level (Muecke et al., 1972; Serralheiro, 2003; Janssen et al., 2008; Ávila et al., 2012; Meireles et al., 2013; Ávila et al., 2015a). Thus, Santa Maria is an ideal place to test competing models for the origins of ocean island uplift. Here we combine detailed fieldwork and $^{40}Ar/^{39}Ar$ geochronology to track relative sea-level change throughout the island's lifetime in order to reconstruct the history of vertical movements affecting the island edifice. We then discuss the plausible mechanisms behind uplift, taking into account the geotectonic context in which the island is located. Finally, our study offers, for the first time, a detailed reconstruction of the evolutionary history of Santa Maria with respect to the magnitude and timing of its vertical movements, and a discussion on their possible origins.

GEOLOGICAL BACKGROUND

Santa Maria Island within the Azores Archipelago

The Azores Archipelago is a group of oceanic volcanic islands located in the mid-North Atlantic. The islands rise from a large, triangular-shaped bathymetric anomaly – the Azores Plateau – straddling the triple junction between the North American (NA), Eurasian (Eu) and Nubian (Nu) lithospheric plates (see Fig.1A) (Lourenço et al., 1998; Gente et al., 2003; Miranda et al., 2016). Two of the Azorean islands – Flores and Corvo – sit west of the Mid-Atlantic Ridge (MAR), whilst the remaining seven islands sit to the east of the MAR, along the diffuse plate boundary between Eu and Nu. The Azores are therefore situated in a complex tectonic setting, essentially governed by traction forces associated with seafloor spreading along the MAR, and right lateral transtensional stress between Eu and Nu (Madeira and Ribeiro, 1990; Madeira and Brum da Silveira, 2003; Vogt and Young, 2004; Gente et al., 2003; Hipólito et al., 2013; Marques et al., 2013; Madeira et al., 2015; Miranda et al. 2015; Miranda et al. 2016). The boundary between these two plates is diffuse, and deformation is presumably being accommodated along a ~140 km–wide shear zone of oblique extensional deformation bounded in the west by the MAR, in the north by the Terceira Rift (TR), and fading out to the south along a line that connects the MAR to the Gloria Fault (GF), passing just south of Faial, Pico and possibly Santa Maria (Hipólito et al., 2013; Marques et al., 2013). In the past, however, the Eu/Nu plate boundary in the region probably was located further south, along the East Azores

Fault Zone (EAFZ), a right lateral transform fault that connected the GF with the MAR (Laughton and Withmarsh, 1974; Searle, 1980; Madeira and Ribeiro, 1990; Luis et al, 1994; Luis and Miranda, 2008). The EAFZ, however, seems to have become inactive some time in the past, judging from its current seismic inactivity (Krause and Watkins, 1970; Searle, 1980). The Azores Triple Junction (and consequently the Eu/Nu boundary) therefore is inferred to have gradually migrated northwards to its present position (Searle, 1980; Luís et al., 1994; Vogt and Jung, 2004; Luís and Miranda, 2008; Marques et al., 2013; Miranda et al. 2015; Miranda et al., 2016). At an early stage (8–4 Ma), this transition took place through the development of the incipient Princess Alice Rift (PAR), followed by a ridge-jump to the more northerly TR at around ~4 Ma, eventually placing Santa Maria at the southern edge of the diffuse Eu/Nu boundary (Miranda et al. 2015; Miranda et al., 2016).

The excess magmatism that gave rise to the Azores Plateau and island edifices is generally regarded as the result of melting associated to an anomalously hot and/or wet mantle beneath the region (Schilling et al., 1975; Bonatti et al., 1990; Asimow et al., 2004; Beier et al., 2012; Métrich et al., 2014). In detail, however, opinions still diverge on the driving mechanism behind this melting. Traditionally, Azorean magmatism has been viewed as resulting from a hotspot-ridge interaction, drawing excess heat from a mantle plume presently centered in the vicinity of Terceira Island (Gente et al., 2003; Madureira et al., 2005, Saki et al., 2015). However, this "hotspot" model has been challenged, with magmatism alternatively being attributed to the existence of a "wetspot" (Métrich et al., 2014), or to volatile-induced melting without involving a hot mantle plume (Schilling et al., 1975; Bonatti et al., 1990).

Santa Maria is the southeasternmost island in the Azores, sitting close to the convergence between the TR, the GF, and the EAFZ (see Fig.1A). The island is located on the eastern edge of the Azores Plateau, resting on lithosphere that is 35–45 Ma old (Gente et al., 2003; Luis and Miranda, 2008; Miranda et al. 2015; Miranda et al. 2016). Rising from the -2500 m isobath, Santa Maria's volcanic edifice presently reaches 587 m in elevation at Pico Alto, its highest point. Morphologically, the island edifice is extremely asymmetric both above and below sea level (Fig, 1B). Below sea level, the insular shelf that surrounds the island is much wider and deeper on the northern side than on the remaining sides. Effectively, the shelf edge in the north is at -120 m to -180 m and is located up to 6–7 km offshore (cf. Fig 1B); in contrast, along the remaining sides, the same morphological feature can be found between -40 m and -80 m and usually extends less than 1.5 km offshore (Ávila et al., 2008). In a similar fashion, the island's topography is also asymmetric, featuring a stepped, west-sloping low-relief plateau on the western (windward) side, in stark contrast with the higher, more mountainous eastern (leeward) portion of the edifice. Coastlines generally correspond to high plunging cliffs, with rare small, perched sand/gravel beaches along adjacent protected bays (e.g. at Praia Formosa or at São Lourenço).

Santa Maria's geological history

Santa Maria is the oldest island edifice in the Azores Archipelago, having emerged above sea level sometime during the Late Miocene (Abdel-Monem et al., 1975; Féraud et al., 1980; Féraud et al., 1981; Serralheiro et al., 1987; Storetvedt et al., 1989). Based on previous studies (e.g. Agostinho, 1937; Zbyszewski and Ferreira, 1960; Serralheiro et al., 1987; Serralheiro and Madeira, 1990; Serralheiro, 2003; Ávila et al., 2012; Meireles et al., 2013; Sibrant et al., 2015a), and using the general stratigraphic scheme defined by Serralheiro et al. (1987) and Serralheiro (2003), the overall geological history of the island could be summarized (Fig. 2) as follows: (i) emergence of the volcanic edifice above sea level sometime during the Late Miocene (the Cabrestantes and Porto Formations); (ii) formation of a basaltic shield volcano during the Late Miocene/Early Pliocene (the Anjos Volcanic Complex); (iii) subsequent truncation of the shield volcano by subaerial and marine erosion, with deposition of terrestrial and marine sediments and synchronous submarine volcanic activity on the eastern side of the island during the Early Pliocene (the Touril Volcano-sedimentary Complex); (iv) re-emergence of the volcanic edifice by increased volcanic activity, initially exclusively submarine and later subaerial, forming a NNW-SSE trending volcanic ridge during the Early Pliocene (the Pico Alto Volcanic Complex); and (v) erosion followed by low volume post-erosional volcanic activity, forming a set of monogenetic magmatic and hydromagmatic cones, and associated pyroclastic and effusive sequences, during the Late Pliocene (the Feteiras Formation); (vi) uplift and erosion of the edifice from Late Pliocene to the present. Sibrant et al. (2015a) also propose a sequence of substantial flank collapses to the east, each at the end of the two main building stages of island evolution.

Despite the fact that the succession of first-order events in Santa Maria's history has been generally understood – and broadly constrained by the modern K/Ar geochronology dataset of Sibrant et al. (2015a) – several key aspects in its evolutionary history remain to be clarified. The first and most important one concerns the magnitude, timing, and origins of its uplift/subsidence history. Previous studies have made general inferences about these movements, but none has so far presented a systematic analysis on the subject, or tried to understand the mechanisms behind such movements. The second aspect concerns the concise timing of emergence for the first island edifice. Using K/Ar geochronology, Abdel-Monem et al. (1975), Féraud et al. (1980), and Féraud et al. (1981) suggested contrasting ages of ~8.12 and ~5.5 Ma, respectively, for the onset of subaerial volcanism, with the latter age bound being ~5.7 Ma, recently confirmed by Sibrant et al. (2015a). However, none of these studies tried to date the hydromagmatic Cabrestantes Fm, which constitutes the seemingly oldest preserved evidence for island emergence (despite its very limited outcrop expression). Also, the definition – and consequently its stratigraphic/cartographic identity – of the Feteiras Fm is still poorly constrained, as Sibrant et al. (2015a) pointed out. Finally, so far little is known about the concise, stratigraphically bound, geochemical evolution of the island edifice and its parental magmas. This paper aims to address the first two aspects, further contributing to our knowledge on Santa Maria's evolutionary history, and the geodynamic evolution of the Azores in general.

METHODOLOGY

Sampling of uplift tracers

The island's volcanostratigraphic succession was studied in detail to identify the highest position of relative sea level within each of the main stratigraphic units, and to gain insight on the overall evolutionary history of the edifice. Ample use of exposures along the coastal cliffs was made, using several boat trips to document the first- and second-order stratigraphic relations exposed around the full circumference of the island. Whenever necessary, the elevation of individual horizons (relative to present sea level) was measured using an Impulse 200LR laser distance meter produced by Laser Technologies, Inc.™, with a range up to 500 m. This equipment was also used to estimate the apparent vertical displacement of faults, by measuring the elevation difference between easily identifiable marker horizons that occur on fault counterparts.

Uplift tracers used in this study corresponded to palaeo sea-level markers, as defined by Ramalho et al (2010a,b,c) and Ramalho et al. (2011). Priority was given to targets representing the passage zone between subaerial and submarine lava flows within effusive lava deltas, since this feature marks very accurately the contemporaneous position of sea level (Jones and Nelson, 1970; Cas and Wright, 1987; Porebski and Gradzinski, 1990; Ramalho et al., 2010a,b,c; Ramalho, 2011; Meireles et al., 2013). After carefully selecting the dating targets, samples were collected for later analysis in the laboratory.

Tracing of Plio-Quaternary shorelines

The geomorphology of Santa Maria was analyzed in detail in order to map the position of each of the Plio-Quaternary marine terraces found on the island. Consequently, we traced the outline of the inner edge of each terrace (i.e. the shore angle coeval to each palaeo-shoreline) using stereoscopic aerial photo interpretation (color vertical imagery from 09/2005, at an approximate scale of 1:18,000) and a 2-m spatial resolution Digital Elevation Model (DEM) generated from a 1/5,000-scale altimetric database. This exercise was later complemented with field observations and localized differential GPS surveys, in order to determine the position and elevation of the inner edges with greater precision and accuracy. Additionally, trenches were dug in order to prove the presence of marine sediments at a selected terrace, and to recover dateable material. Our palaeo-shoreline reconstructions were then plotted in the same 2-m spatial resolution DEM.

$^{40}Ar/^{39}Ar$ geochronology

The $^{40}Ar/^{39}Ar$ analyses were performed at the USGS in Denver, CO. Fresh rock fragments (~1 mm^3) free of obvious alteration and mineral grains of sanidine were prepared using crushing, picking, and heavy liquid techniques. The basalt samples were irradiated for 0.5 MWh and the sanidine sample was irradiated for 0.17 MWH in the central thimble position of the USGS TRIGA reactor (Dalrymple et al., 1981), while also being rotated at 1 rpm. Following irradiation, the basalt fragments and sanidine samples and standards were loaded with tweezers to a stainless steel sample holder and then placed into a laser chamber with an externally pumped ZnSe window. The volume of the mostly stainless steel vacuum line extraction line, including a cryogenic trap operated at -130°C and two SAES™ GP50 getters (one room temperature, one operated at 2.2A), is estimated at ~450 cc. A combination of turbo molecular pumps and ion pumps maintain steady pressures within the extraction line of $< 1 \times 10^{-9}$ Torr. Samples were incrementally heated in steps of 90 seconds, by controlled power output of a 50W CO_2 laser equipped with a beam homogenizing lens resulting in uniform energy over the entire sample surface. During laser heating any sample gas released was exposed to the cryogenic trap and was further purified for an additional 120 seconds by exposure to both the cryogenic trap and the SAES getters. The sample gas for all basalt samples was expanded into a Thermo Scientific ARGUSVI™ mass spectrometer and argon isotopes were analyzed simultaneously using 4 Faraday detectors (^{40}Ar, ^{39}Ar, ^{38}Ar, ^{37}Ar) and 1 ion counter (^{36}Ar). Analytical data for the one sample of sanidine unknowns (SMA07) was analyzed by peak hopping on an electron multiplier in analog mode on a Mass Analyser Products™ 215-50 mass spectrometer. Following data acquisition of 10 minutes, time zero intercepts were fit to the data (using parabolic and/or linear best fits) and corrected for backgrounds, detector inter-calibrations, and nucleogenic interferences. The Masspec computer program written by A. Deino of the Berkeley

Geochronology Center was used for data acquisition, age calculations, and plotting. All $^{40}Ar/^{39}Ar$ ages reported in Table 1 are referenced to an age of 28.201±0.046 Ma for the Fish Canyon sanidine (Kuiper et al., 2008), the decay constants of Min et al. (2000), and an atmospheric $^{40}Ar/^{36}Ar$ ratio of 298.56±0.31 (Lee et al., 2010). Laser fusion of >10 individual Fish Canyon Tuff sanidine crystals at each closely monitored position within the irradiation package resulted in neutron flux ratios reproducible to ≤ 0.25% (2σ). Isotopic production ratios were determined from irradiated CaF_2 and KCl salts and for this study the following values were measured: $(^{36}Ar/^{37}Ar)_{Ca}$ = (2.45±0.05) x10^{-4}; $(^{39}Ar/^{37}Ar)_{Ca}$ = (6.59±0.10) x10^{-4}; and $(^{38}Ar/^{39}Ar)_K$ = (1.29±0.03) x10^{-2}. Cadmium shielding during irradiation prevented any measurable $(^{40}Ar/^{39}Ar)_K$. $^{40}Ar/^{39}Ar$ plateau ages (and uncertainties) are considered the best estimate of the age of the basalt samples and were calculated from samples if three or more consecutive heating steps released ≥ 50% of the total ^{39}Ar and also had statistically indistinguishable $^{40}Ar/^{39}Ar$ ages. If samples nearly met these criteria, a preferred weighted mean age was calculated, otherwise the integrated age is used as the preferred age of the basalt. For samples dated by single crystal laser $^{40}Ar/^{39}Ar$ fusion, a weighted mean was calculated from grains considered to represent a single age population and excluded any clear outliers.

Uplift reconstructions

Uplift reconstructions were made using the method established by Ramalho et al. (2010a,c) and Ramalho (2011). Accordingly, a comparison between relative sea-level positions and coeval eustatic sea level was established in order to infer vertical displacements and reconstruct uplift/subsidence trends. The Miller et al. (2005) eustatic curve was used as a reference since it is one of the few curves that spans the ~6.5 Ma time interval required for this study. Uncertainties in sea level, as well as the effects of glacio-isostatic adjustment in relative sea level, were not factored in this first-order approximation. This is so because our reconstructions span several million years and the majority of the relative sea-level markers used in this study correspond to volcanic tracers that could have been formed at any given time within a glacio-eustatic cycle. Additionally, since some of the chosen uplift tracers were vertically offset by local faults, a "tectonic correction" was applied to those tracers located on adjacent downthrown blocks; this was done simply by adding the apparent vertical fault displacement into their elevation, in order to minimize local tectonic effects on relative sea-level differences. This "tectonic correction", however, was only applied to uplift tracers located within a short distance to each other, and not to tracers located in different parts of the island, because we have less control of vertical tectonics at that scale. Finally, all elevation values are given in meters above or below (when preceded by "-") present mean sea level (local datum).

RESULTS

Uplift tracers

Cabrestantes and Porto Fms

The outcrop at Ribeira dos Cabrestantes corresponds to the eroded remains of a surtseyan cone, implying an eruption from a vent located in shallow water. It is not known for certain whether this outcrop corresponds to the submarine base of the cone or its emergent (subaerial) summit, i.e. it is not possible to assert with precision where coeval sea level was at the time of its extrusion. However, the tuffs are generally even- and planar-bedded, without any cross-stratification, bomb sags, or other signs of surge deposition and subaerial ballistic impacts. Consequently, we are inclined to interpret this outcrop as water-settled and therefore suggest that coeval sea level was probably above the eroded top of the present outcrop. We therefore assign an elevation of 37 m as a first-order approximation for coeval relative sea level. In order to constrain the age of this cone, two samples (SMA10 and SMA11) corresponding to two different volcanic bombs were collected at this site.

The cones of Porto Fm (sensu Serralheiro et al., 1987) correspond to strombolian vents and therefore were erupted subaerially. Their presence, together with the outcrop at Cabrestantes, attests to the transition from submarine to subaerial volcanism during island emergence. The fact that these occur at the same elevations as Cabrestantes shows that there was probably a small relative sea-level change (lowering of sea level) in between the extrusion of these units, confirmed by the transition between surtseyan and strombolian volcanism.

Anjos Volcanic Complex

As reported by previous authors (e.g. Serralheiro et al., 1987; Serralheiro, 2003; Ávila et al., 2012), the exposed Anjos volcanic edifice is overwhelmingly subaerial in nature. At Ilhéu da Vila (Fig. 2) and Baía do Mar da Barca, however, it is possible to find submarine morphologies intercalated within the subaerial sequence. These mark the position of sea level during one or two distinct moments during the extrusion of the shield volcano and therefore constitute ideal targets to track uplift/subsidence. The sequence is particularly clear at Ilhéu da Vila, where a former coastline is preserved at ~11 m in elevation (Fig. 3A). Here, a shore platform carved on subaerial flows is overlain by a boulder beach, which is in turn covered by a thick subaerial lava flow whose base entered in the water, generating pillowed structures. This passage zone therefore demarks the position of sea level during the extrusion of the lava flow, and so was sampled for geochronology (sample SMA36). The sequence at Baía do Mar da Barca marks relative sea level at approximately the same elevation. As for the rest of Anjos Volcanic Complex, relative sea level was well below present sea level, perhaps suggesting that these submarine morphologies were formed during short-lived glacio-eustatic highstands when relative sea level was particularly high.

Touril Volcano-Sedimentary Complex

The Touril Volcano-sedimentary Complex (Figs. 3B–D) corresponds to a dominantly clastic sedimentary sequence (conglomerates, sandstones, calcarenites and rare limestones) intercalated by hydromagmatic tuffs and submarine effusive products (particularly on the eastern side of the island). This thick sequence varies laterally and vertically in characteristics but in general grades from coarser terrigenous conglomerates in the lower part of the succession towards finer fossiliferous marine conglomerates, sandstones, calcarenites and limestones, near the top of the succession (Serralheiro, 2003; Ávila et al., 2012). In other words, this sequence tends to pass from highly energetic terrigenous sediments at the base to an increasingly open marine character towards the top, as also reflected in its fossil content (e.g. Serralheiro, 2003; Janssen et al., 2008; Ávila et al., 2012; Ávila et al., 2016). This transition suggests that relative sea level gradually rose throughout the time period spanned by this unit; although we did not quantify in detail this relative sea-level change, we may infer it was in excess of 70–80 m, as this is the maximum thickness attained by the sequence. The maximum elevation at which Touril presently occurs is ~120 m. A single sample was collected in this unit (SMA02), corresponding to the pillow lavas that form the base of the sequence (at 8 m in elevation) of Pedra-que-pica/Ponta do Castelo, described later in this text.

Pico Alto Volcanic Complex

The Pico Alto Volcanic Complex makes the bulk of the eastern part of Santa Maria's volcanic edifice, being very rich in relative sea-level markers that are superbly exposed along the island's southern, eastern, and northern coastal cliffs (Figs. 3B–F and 4A–B). This unit is largely composed of effusive sequences with submarine characteristics at the base – with occasional intercalated marine sediments – and subaerial characteristics at higher elevations. The passage zone between the submarine and subaerial products in these sequences varies in elevation across the island but is generally located in between ~60 and ~200 m, and it is generally found at increasingly higher elevations towards the eastern and western fringes of the volcanic edifice (see Fig. 2B). The internal structure of Pico Alto Volcanic Complex shows that, in the southern, northern, and western parts of the island, the underlying sedimentary sequence of Touril has been overlain by thick lava-fed delta sequences, either exhibiting the typical prograding "pillow and hyaloclastite" Gilbert-type structure, or more rarely as aggradational lava-fed deltas composed of submarine sheet flows (for details on these types of lava-fed deltas see Ramalho et al. 2013). The contact between the Touril and the Pico Alto sequences in these areas is relatively flat, very gradually dipping towards the eastern part of the island, where it disappears below sea level. In contrast, in the eastern part of the island, the structure of Pico Alto Volcanic edifice almost exclusively corresponds to extensive "pillow and hyaloclastite" Gilbert-type lava-fed deltas, consistently prograding to the eastern quadrant; all across the area, the steeply-dipping "foreset units" of these lava-fed deltas extend continuously from their passage zone at elevations up to ~130 m down to present sea level. In places, however, younger lava-fed deltas lie conformably or unconformably above the initial lava delta sequence, providing additional information on relative sea-level change. Since the passage zone in all these lava deltas very accurately marks where relative sea level was at a given point of the history of Pico Alto volcanic edifice, several key sections were selected and studied in detail, in order to get a representative overview of relative sea-level change during this phase of the construction of the island.

Monte Gordo/Monte das Flores. All across the western part of the Pico Alto volcanic edifice the structure corresponds to westward-prograding Gilbert-type lava-fed deltas, either lying directly over the Touril marine sediments, or above a thin set of laterally very extensive submarine sheet flows that cap the Touril sequence. The passage zone in these lava deltas is generally at 180–200 m, corresponding to the highest elevation at which this sea-level marker occurs within the Pico Alto edifice. The sequence is particularly well exposed around Monte Gordo and Monte das Flores in the northern part of the island (see Figs. 2 and 3B), where the passage zone can be seen at ~200 m; samples SMA18 and SMA45 were collected in the submarine lava flows immediately below this passage zone, in Monte Gordo, and constitute the highest, directly dateable palaeo sea-level marker in Santa Maria.

Ponta do Pesqueiro Alto. Immediately to the east of Monte Gordo, along the northern coast, the same passage zone is located at ~130 m in elevation, due to the 60–70 m vertical displacement of Cré Fault; this passage zone, however, can be traced several kms to the east, to Ponta do Pesqueiro Alto (Fig. 3C), where it still occurs at ~130 m. The sequence, in this place, exhibits a tabular stacking of marine conglomerates, submarine flows, and marine sediments belonging to the Touril Complex, covered by a northward-prograding Pico Alto lava delta, with a very clear passage zone.

Ponta do Norte. Also in the northern coast, at Ponta do Norte (Figs. 3D and 4A), two lava delta sequences overlap unconformably (with marine sediments intercalated in between them); whilst the foresets of pillow lavas (dipping to ENE) of the older lava delta reach up to

~100 m in elevation (being truncated atop), the younger lava delta exhibits its passage zone at 110 m, where sample SMA30 was collected. This peninsula, however, is ~50 m downthrown relatively to the island's mainland, along the vertical fault that separates these two blocks (see Fig. 2).

Ponta do Morgado/Ponta do Cedro. The stretch of coast that extends from the southern end of Baía de São Lourenço to Ponta do Cedro possibly constitutes one of the best exposures in the island. This entire stretch of coast corresponds to a long-lived Gilbert-type lava-fed delta, prograding to the east, whose passage zone is located in between ~80 m (in the inner part of the delta, e.g. within Baía do Cura) and ~130 m (in the outer part of the delta, e.g. Ponta do Morgado, Fig.4B).

Ponta do Castelo. At Ponta do Castelo (Fig. 3E), the southeasternmost tip of the island, two conformably overlapping lava delta sequences constitute two relative sea-level markers at 55 m and 90 m, where samples SMA09 and SMA08 were collected, respectively (for more details on these sequences refer to Meireles et al., 2013 and Ávila et al., 2015a,d). Sample SMA02 was also collected at the pillow lavas that form the base of the sequence (at 8 m in elevation), at Pedra-que-pica, which correspond to the top of the Touril Complex. The sequences at Ponta do Castelo and Pedra-que-pica are, however, displaced by a set of faults whose total apparent vertical displacement corresponds to 12 m of relative downthrow to the E.

Ponta da Malbusca**.** Finally, at Ponta da Malbusca (Fig. 3F) in the southern coast, the sequence comprises a subhorizontal pile of pillow lavas, marine sediments (both belonging to the Touril Complex), and submarine sheet flows, which transitions to subaerial flows and tuffs approximately at 130 m. The overall Pico Alto sequence in this area corresponds to an aggradational lava-fed delta, generated by the vertical stacking of thick and laterally extensive submarine sheet flows and subordinate marine sediments, accompanied by a relative sea-level rise of at least 60 m (Rebelo et al., in review). Sample SMA03 was collected in the highest submarine lava flow in the sequence, in order to date this relative sea-level tracer.

Feteiras Fm.

The Feteiras Fm correspond to a set of monogenetic hydromagmatic and magmatic cones (and associated products), mostly concentrated on the central part of the island, which corresponds to a broad plateau at the foot of the Pico Alto range. This plateau has been interpreted as a Pliocene marine terrace, presently located at 200–230 m in elevation, over which these cones were extruded (Serralheiro et al., 1987; Serralheiro, 2003; Ávila et al., 2012). Therefore, in order to get an upper bound on the age of this surface, samples SMA28 and SMA29 were collected at the cones of Monteiro and Saramago, respectively (cf. Fig. 2A). Since the products of this volcanic stage have been mapped by Serralheiro et al. (1987) down to ~130 m, the age of these cones (at least the youngest) could also be used as a first-order approximation to the minimum age of any marine terraces above that elevation.

Plio-Quaternary shoreline reconstructions

Our geomorphological reconstructions revealed the presence of 10 recognizable uplifted palaeo-shorelines at approximately 7–11 m, 45–50 m, 55–60 m, 65–70 m, 85–90 m, 105–110 m, 120–125 m, 140–145 m, 155–165 m and 210–230 m in elevation (see Figs. 4C and 5). The succession of marine terraces and the resulting staircase morphology is particularly evident on the NW slope of the island, from Anjos towards Monte Gordo and Monte das Flores, and also in the SW, from Ponta do Marvão towards Pico do Facho (see Fig. 5). The uncertainty in our reconstructions naturally increases with elevation, due to increasingly more severe topographical decay, and later volcanic cover. The position and outline of the higher 210–230 m palaeo-shoreline is particularly poorly constrained, and is crudely estimated by a marked slope break (and morphology contrast) at the foot of the Pico Alto range. In a similar fashion, due to anthropic landscape alterations, the area surrounding Santa Maria's airport is equally problematic. In contrast, the position and outline of the lower Marine Isotope Stage (MIS) 5e shoreline is well constrained and has been the subject of previous studies in the Azores (e.g. Ávila et al., 2009; Ramalho et al., 2013; Meireles et al., 2013; Ávila et al., 2015c,d). The range in elevation of MIS5e notches and terraces in Santa Maria is further constrained by studies of the same highstand elsewhere around the world (e.g., Hearty et al., 2007; O'Leary et al., 2013).

The lack of well-developed marine terraces (other than MIS5e) on the southeastern, eastern, and northeastern sides of the island is noteworthy. However, in several places along these coastlines, wave-cut notches are clearly visible at several elevations across the plunging cliffs, attesting to the relative position of sea level at the above-mentioned elevations. Apart from the ubiquitous MIS5e notches and terraces, which can be observed at several locations all around the island at 7–11 m in elevation, rarer (and presumably older) notches have also been recorded at 18–20 m (e.g. at Ponta da Malbusca, and Baía do Cura) or even at 105–110 m (at Ponta do Morgado/Baía do Cura, see Fig. 4B).

Field reconnaissance revealed the presence of loose remains of Pleistocene fossiliferous calcarenites in a small area to the NW of Ginjal, next to the marked inner edge of the +85–90 m palaeo-shoreline, and in accordance with what has been reported by Serralheiro et al. (1987). This place was thus chosen as the site for trenches, which promptly revealed a Pleistocene beach 1 m below the surface. The beach deposits (Fig. 4D) exhibit a basal conglomerate covered by micro-conglomerates of rounded stranded pumice (which was transported to Santa Maria as floatsam from another island) and bioclast-rich sand, featuring typical very shallow foreshore fossil assemblages (e.g. vermetids and limpet shells of the extant *Patella aspera* Röding, 1798). This sequence therefore marks very accurately the relative position of sea level and, since the age of the stranded pumice can be considered penecontemporaneous of coastal deposition (as sea wrack in high tidal area), it provides rare and fortuitous dateable material with which to track quaternary uplift. A pumice sample (SMA07) was thus collected for $^{40}Ar/^{39}Ar$ geochronology.

$^{40}Ar/^{39}Ar$ geochronology

Our $^{40}Ar/^{39}Ar$ geochronology results for Santa Maria's volcanic relative sea-level tracers range from 6.01±0.14 Ma to 2.92±0.08 Ma (Fig. 6 and Table 1; age uncertainties 2σ throughout). The surtseyan deposits of Cabrestantes Fm yielded 6.01±0.14 Ma and 5.8±0.3 Ma, results that overlap within their uncertainty envelop; given the larger uncertainty in the latter value, we assume the former to be a stronger age constraint for this sea-level tracer. These ages confirm the significance of this spatially restricted outcrop as the oldest unit in the island. The $^{40}Ar/^{39}Ar$ age of 5.84±0.09 Ma for the palaeo-coastline within the subaerial Anjos shield volcano, at Ilhéu da Vila, is in reasonable agreement with the 5.70±0.08 Ma age reported by Sibrant et al. (2015a) for the subaerial flows just opposite the channel on mainland Santa Maria. The three relative sea-level markers from Pedra-que-pica/Ponta do Castelo cross-section yielded, respectively from the base to the top, 4.78±0.13, 4.13±0.19, and 3.98±0.05 Ma. These values provide a very consistent timing for the formation of such transgressive sequence. The latter result is also in agreement with the 3.96±0.06 Ma reported by Sibrant et al. (2015a) further west of Ponta do Castelo. Our sea-level marker at Ponta da Malbusca yielded 4.08±0.07 Ma, which is also in good agreement with the 4.02±0.06 Ma reported by Sibrant et al. (2015a) for the underlying upper submarine part of the sequence. Taken together, these results once again show that this volcano-sedimentary sequence was deposited rapidly during a transgressive period in between 4.32 and 4.0 Ma, in perfect agreement with field stratigraphy. The two samples collected at the lava delta sequence of Monte Gordo yielded two consistent ages of 3.71±0.08 and 3.63±0.09 Ma, providing a solid age estimate for this sea-level tracer. Farther east, the lava delta sequence at Ponta do Norte yielded 3.52±0.04 Ma; since this sequence unconformably rests on a former insular shelf carved on older similar structures belonging an earlier stage of Pico Alto volcanic complex, it provides an age constraint on late volcanic progradation. Finally, the post-erosional cones of Saramago and Monteiro yielded, respectively, 2.92±0.08 and 3.22±0.13 Ma; the latter result, however, contrasts with the age of 3.52±0.05 Ma reported by Sibrant et al. (2015a) for the same structure.

Single sanidine grains extracted from the pumice at Gingal (sample SMA07) yielded an age probability plot consistent with an $^{40}Ar/^{39}Ar$ age of 2.15±0.03 Ma. We therefore consider an age of 2.1–2.2 Ma for the eruption of this pumice and consequently the same approximate age for its stranding along the coeval coastline at Santa Maria.

Uplift reconstructions

Our uplift/subsidence reconstructions are presented in Fig. 7, which allows the correlation between the relative position of sea level for each of the dated tracers and the global mean glacio-eustatic sea level. These correlations show that the position of relative sea-level tracers increase in elevation with increasing age, back to 3.5–3.7 Ma, when the trend is reversed. Therefore, our reconstructions show that Santa Maria experienced a slow uplift (of ~60 m/Ma) trend in the last 3.5–3.7 Ma, being preceded by a faster subsidence trend (of ~100m/Ma), which started around 5.8 Ma. The minimum estimated total vertical displacement experienced by Santa Maria is solidly bounded by the ~3.7 Ma passage zone at Monte das Flores lava-fed delta, at an elevation of ~200 m; a weaker bound is provided by the inferred marine terrace at 210–230 m in elevation, with a probable age between 3.7 Ma (age of the underlying volcanic sequence) and 3.2 Ma (age of the oldest Feteiras cone). Therefore, and using the more solid bound, the minimum total vertical displacement corresponds to +180 m, since this is the elevation difference between the passage zone at Monte das Flores and their contemporaneous sea-level highstands (see Fig. 7). If, instead, the long-term (averaged) sea-level curve is used as a reference (smoothed black line in Fig. 7), the estimated total vertical displacement corresponds to approximately +205 m, accordingly. As for the preceding sea-level markers, if one subtracts the +180 m of post-Pico Alto minimum vertical displacement inferred above, most of them would fall well below their contemporaneous sea-level minima, at increasingly lower positions with increasing age. This, therefore, attests to the inferred subsidence trend. Moreover, and considering that the palaeo-coastline at Ilhéu da Vila dates to 5.84 Ma and is presently located at 11 m, the subtraction of 180 m of posterior uplift would bring this lower palaeo-marker to an elevation of -169 m, which represents a negative vertical displacement in excess of 110 m below contemporaneous sea-level minima. If, on the other hand, one considers that this palaeo-coastline was instead formed during a highstand (more likely), the inferred subsidence is in excess of 190–200 m. Finally, it becomes almost impossible to constrain with precision what vertical movements existed in between the Cabrestantes and the Anjos sea-level markers, as elevation difference between them is small enough to fall within the coeval eustatic amplitude and age resolution is not precise enough to assert their exact position within the eustatic curve.

DISCUSSION

Geochronology results

The $^{40}Ar/^{39}Ar$ geochronology results reported here are in general agreement with the ages reported by Feraud et al. (1980), Feraud et al. (1981), Storetvedt et al. (1989) and Sibrant et al. (2015a). Our results, however, provide a more solid constraint on the timing of first emergence above sea level by the island edifice, and refine the existing time constraints on the several volcanic stages that took place to shape this edifice. More importantly, these results allow us to formulate a much clearer picture on the vertical movements affecting the island edifice throughout its evolutionary history, and how those movements affected that evolution.

Uplift reconstructions

The uplift reconstructions here presented, albeit subject to some uncertainty, clearly demonstrate that Santa Maria experienced a complex vertical motion history. This history is characterized by an uplift trend in the last ~3.5 Ma, preceded by a subsidence trend of similar magnitude, which started almost as soon as the island emerged. Despite the relative lack of dateable sea-level tracers spanning the last 3.5 Ma – which precludes any more precise uplift rate calculations – the inferred uplift trend is also clearly attested by the staircase of marine terraces present on the western side of the island (and the notches on the eastern side), and by the remains of a Pleistocene beach in one of those terraces, at 85-90 m in elevation. The preceding subsidence trend is more tightly constrained, on account of a richer record provided by the numerous passage zones of Pico Alto and Anjos lava deltas. This subsidence trend is equally attested by the thick transgressive sequence of the Touril Complex, whose facies variation gradually increases in its more open marine character towards the top.

Implications for island evolution

Our work shows that Santa Maria Island first emerged by surtseyan activity around 6 Ma ago (Fig. 8), as attested by the age of the Cabrestantes Fm. This foundational stage in the island evolutionary history was followed by a transition to the subaerial environment, initially through additional monogenetic volcanism (as attested by the strombolian cone structures of the Porto Fm), then through subaerial shield volcanism. The consolidation of the island edifice was thus sustained by an increase in magma production rates, which led to the formation of a shield volcano (corresponding to the Anjos Volcanic Complex) 5.8–5.3 Ma ago. The resulting shield volcano possibly extended much further to the north and east, as the volcanic structure and the northward extent of the present-day insular shelf both suggest. Whilst the northern side of the existing edifice was probably truncated by marine erosion, the retreat of the eastern side has been tentatively attributed to a flank collapse by Sibrant et al. (2015a). It was also probably at around this time that the edifice entered a period of pronounced subsidence. This subsidence trend was possibly driven by surface loading imposed by vigorous volcanic activity since its magnitude is about 4 or 5 times the expected thermal subsidence (e.g. Stein and Stein, 1992) for that period. Although subsidence rates determined by this study are also an order of magnitude lower than those measured by recent GPS studies (Trota, 2008; Catalão et al., 2011; Miranda et al., 2012; Marques et al., 2013), they are of the same order of magnitude with long-term determination of subsidence in the Azores by morphological proxies such as the shelf break depth (Quartau et al., 2014, 2015, 2016).

Subsequently to the extrusion of the Anjos shield volcano, the edifice entered a period of waning volcanism and erosion, which – aided by subsidence – resulted in the complete or almost-complete truncation of the existing island edifice to form a guyot (Fig. 8). This is well attested by the very flat unconformity between the Anjos and the Touril sequences, which can be followed semi-continuously from Praia Formosa to Baía do Tagarete, across the western side of the island. This period – and its contemporaneous sedimentation – is also well expressed in the stratigraphic succession of Touril Volcano-sedimentary Complex, which grades from high-energy terrigenous coarse sediments, to finer bioclastic sediments with a clear open marine character (Serralheiro, 2003; Ávila et al., 2012; Ávila et al., 2016). As the gradual destruction of the Anjos edifice progressed and the deposition of Touril complex continued, Santa Maria's edifice started to resemble a wide, shallow-water sandy shoal punctuated by occasional residual islets or surtseyan cones; sporadic volcanic activity was entirely submarine in nature and was mostly concentrated in the eastern part of the edifice (Ávila et al., 2012, Ávila et al., 2016). This scenario is clearly attested by the fact that the thick sequence of Touril forms an almost continuous belt that can be followed around the island (except on the eastern side, where it disappears below present sea level), and by the fact that thick submarine effusive products of the subsequent volcanic stage invariably cover this sequence. Moreover, it is also supported by the rich marine fossil record of the Touril Complex, which includes bones of cetaceans (Estevens & Ávila, 2007; Ávila et al., 2015b), teeth of sharks (Ávila et al., 2012) and of bony fishes, coralline algae (e.g. rhodoliths; Meireles et al., 2013, Rebelo et al., 2014; Ávila et al., 2015a,d; Ávila et al., 2016), and a large spectrum of marine invertebrates, e.g., molluscs, echinoderms, bryozoans, foraminiferans, and crustaceans (e.g. Kirby et al. 2007; Madeira et al, 2011; Meireles et al., 2013, Rebelo et al., 2014; Ávila et al., 2015a,d; Ávila et al., 2016). Also, the present-day inclined geometry of the Touril Complex (and the unconformity at its base) may denote a slight eastwards tilting of the island edifice, possibly owing to the off-centered loading of the Pico Alto volcanic edifice (see Fig. 2).

The next stage in the evolution of Santa Maria corresponds to the construction of the Pico Alto volcanic edifice, centered on the eastern side of the island. This stage probably started at ~4.1 Ma and lasted up to ~3.5 Ma. The continuous exposures along the coastal cliffs of the island clearly show that the Pico Alto volcanic edifice started as being entirely submarine, and eventually breached sea level as the edifice grew and volcanic aggradation outpaced subsidence. Effectively, the Pico Alto volcanic succession essentially comprises submarine volcanic sequences and submarine volcanic morphologies, which only pass to subaerial at higher elevations. The fact that the passage zone of these sequences is generally at higher elevations with decreasing age confirms that the subsidence trend initiated during the previous volcanic phase extended throughout the period spanned by the extrusion of the Pico Alto edifice. The construction of this volcano seems to have been mostly centered along the NNW-SSE fissure-fed central range of Pico Alto, from which the edifice expanded, particularly to the west and east of this feature. The edifice's lateral growth was essentially sustained by the westward and eastward progradation of coastal lava deltas, under a gradual relative sea-level rise driven by subsidence, as attested by the numerous lava-fed delta structures superbly exposed along the island's coastline. Whilst the westward progradation of lava-fed deltas occurred over the existing shoals – leading to the juxtaposition of Pico Alto effusive delta sequences over the Touril marine sediments – the eastwards volcanic progradation extended the edifice beyond the coeval shelf edge, as the vertical extension of the foresets on the eastern effusive deltas nowadays suggest (see Fig. 4B). As for the eastern part of the edifice, the geometry described above is in stark contrast with the one inferred by Sibrant et al. (2015a), which led these authors to suggest that the whole eastern flank of Pico Alto was removed by a large-scale flank collapse at ~3.6 Ma. The architecture of the lava-fed deltas exposed all around the island's coast precisely shows that the overall volcanic structure of eastern Santa Maria dips to the eastern quadrant, and that the eastern flank of the edifice is not all missing. Moreover, the late extrusion of extensive lava-fed deltas unconformably over a well-developed insular shelf on the eastern side of the island – such as in Ponta do Norte, at ~3.5 Ma (Fig. 4A) – shows that eastwards/northwards volcanic progradation was occurring until late in the evolution of Pico Alto, as opposed to what Sibrant et al. (2015a) proposed. The hypothesis for a major flank collapse to have affected the late evolution of Santa Maria Island is therefore rejected. The end of the Pico Alto volcanic phase, nevertheless, represents a major shift in the evolution of Santa Maria, since from this point onwards the island never experienced voluminous volcanism again, and started its remarkable uplift trend that extended to the present day.

The subsequent evolutionary stage in the evolution of Santa Maria is characterized by waning volcanism, erosion, and uplift (Fig. 8). The end of the Pico Alto volcanic phase is poorly constrained, but possibly took place at around 3.5–3.7 Ma. During this period, volcanism experienced a gradual shift from larger fissure-fed eruptions (which had sustained the growth of the edifice and the expansion of coastlines) to smaller monogenetic eruptions, punctuating the island edifice with low-volume magmatic and hydromagmatic cones and associated effusive products (e.g. Pico Maloás at Malbusca, Pico do Facho, Ponta do Norte cone, etc). As volcanic growth waned and became more episodic, erosion gained importance leading to increased topographic decay and coastal retreat. This coastal retreat was particularly pronounced on the western side – the windward side – leading to the formation of broad coastal shelves that became marine terraces as the island gradually continued its uplift trend. Episodic post-erosional monogenetic volcanism (corresponding to the Feteiras Fm) seems to have continued up to 2.8 Ma, partially covering the recently formed higher marine terraces with its products. The late Pliocene therefore marks the end of Santa Maria's volcanic life; the island however, continued to experience uplift until the present day, as attested by the staircase of marine terraces that characterize the morphology of its western slope. This final stage in the island evolution was also accompanied by neotectonic activity, essentially materialized by NNW–SSE (and more rarely NE–SW) nearly vertical dip-slip block faulting, which displaced some of the higher marine terraces (Madeira, 1986; Madeira et al., 2015).

Coastal evolution and marine terrace development

The preferential development of broad marine terraces on the western side of Santa Maria is somewhat intriguing. However, we attribute this asymmetry to a combination of two main factors: stronger marine erosion on the windward side of the edifice, and a favorable lithological structure. The Azores Islands are dominantly exposed to a highly energetic wave regime approaching from the WNW due to the strong westerlies to which the archipelago is exposed (Quartau et al., 2010, 2012; Rusu and Soares, 2012). Marine erosion is therefore significantly stronger on the western and northern sides, partially explaining the existing asymmetry. Effectively, on the eastern side, marine abrasion seems to have been much more limited, leading to the formation of plunging cliffs with occasional wave-cut notches, instead of coastal platforms; the very presence of wave-cut notches at different elevations precisely attests to the very low erosion rates affecting this side. Probably, the development of broad terraces on the western side was also facilitated by the fact that many of the terraces were carved along the softer Touril sequence and the gently dipping contacts between this unit and the underlying Anjos and overlying Pico Alto volcanic edifices. Effectively, the extensive terraces located at elevations between 50 m and 120 m precisely coincide with those interfaces (compare Figs. 2 and 5). In a similar fashion, the generation of the extensive 210–230 m marine terrace was facilitated by the presence of an antecedent flat morphology provided by the top of the western lava deltas of Pico Alto. Thus, in our opinion, the staircase of marine terraces on the western side of the island is the fortuitous product of uplift, stronger marine erosion on the windward side, and a favorable lithological structure. In contrast, on the remaining coasts, the steepness of the plunging cliffs was sustained by low erosion rates (as the geometry of the MIS5e reconstructed shoreline also shows), possibly aided by small-scale mass wasting (rock and debris falls and topples on the steepest cliffs, and rock slides along the layered pillow & hyaloclastite slopes).

Possible uplift mechanisms

Santa Maria's long-lived uplift trend is quite remarkable, on account of the island's geodynamic setting. The island is located on very young lithosphere and therefore should be experiencing considerable thermal subsidence (Parsons and Sclater, 1977; Stein and Stein, 1992). In fact, practically all other Azorean Islands are in a clear subsidence trend, including nearby São Miguel (Muecke et al., 1972; Trota, 2008; Catalão et al., 2011; Miranda et al., 2012; Marques et al., 2013, Miranda et al. 2015); this subsidence probably results from the combined effects of recent volcanic loading (all other islands in the Azores are volcanically active and considerably younger than Santa Maria), thermal subsidence, and vertical tectonics (particularly São Miguel, Terceira, and Graciosa, which are located in the "central graben" of the Terceira ultra-slow spreading ridge). Given this regional context, the uplift trend at Santa Maria cannot be attributed to a regional, wide-ranging mechanism, but rather to a mechanism that acts essentially at a local scale.

A common uplift mechanism affecting several ocean island systems concerns the far-field flexural response of the lithosphere to volcanic loads, as it has been shown to be case of Hawaii and other Pacific archipelagos (e.g. Grigg and Jones, 1997; Zhong and Watts, 2002; Huppert et al., 2015). This mechanism, however, is not applicable to the case of Santa Maria because: a) the only island edifice located at a reasonably suited distance[1] to generate a flexural bulge capable of uplifting Santa Maria is the nearby island of São Miguel, which is considerably younger (<1 Ma, Johnson et al., 1998; Sibrant et al., 2015b) than the onset of the uplift trend here reported; and b) the magnitude of the uplift is far too high to be explained by effects of flexural loading of a nearby island (Ramalho et al., 2010c; Huppert et al., 2015). Isostatic uplift or uplift generated by flexural rebound as result of erosion and mass wasting probably also accounts for only a small fraction of the uplift experienced by Santa Maria. Whilst it is extremely difficult to quantify the amount of material removed by marine and fluvial erosion, it is reasonable to assume that this material got redistributed within the flexural moat of the edifice, greatly attenuating the possible uplift generated by the removal of material from the subaerial part of the island (Smith and Wessel, 2000). Additionally, the occurrence of large-scale mass wasting at the end of the Pico Alto volcanic phase (as proposed by Sibrant et al., 2015a) is not supported by the island's volcanic structure, and therefore cannot account for the uplift reported here, despite the temporal agreement between the proposed age for this hypothetical collapse and the onset of uplift. However, even this hypothesis was considered valid, the uplift response following a

[1] Considering an elastic plate model with flexural rigidity parameters compatible with thin oceanic lithosphere, or even considering a thickened plate due to the addition of the Azores plateau

catastrophic flank failure is expected to have been faster than the slow uplift trend reported here, which extends over a period of 3.5 m.y.

Another mechanism that could be invoked as the source of Santa Maria's slow but long-lasting uplift trend has its roots on the island's geotectonic setting. Santa Maria rises from the southeastern edge of the Azores Plateau, which is a triangular zone limited by the TR to the NE, the EAFZ and PAR to the SW, and the GF to the SE (see Fig.1). At ~4 Ma, the area experienced a tectonic reconfiguration due to the migration of the Nu-Eu plate boundary from the incipient PAR to a location further north, now established as a diffuse plate boundary around the TR (Miranda et al. 2015; Miranda et al. 2016). The area where Santa Maria lies thus became wedged in between the major discontinuities that limit the Azores Plateau to the South and East, and a developing spreading ridge to the NE; this reconfiguration induced by the onset of the Terceira ultra-slow spreading ridge could have resulted in localized uplift, acting to raise the island. However, neotectonic studies along the diffuse Azorean segment of the Eu-Nu boundary point to a transtensional regime in the region since all recognized active faults (both on and offshore) present normal or oblique (normal dextral or normal sinistral) slip (Madeira and Brum da Silveira, 2013; Hipólito et al., 2013; Carmo et al., 2013; Madeira et al., 2015; Carmo et al., 2015). Such a tectonic regime is not compatible with significant tectonic uplift in this region.

In our opinion, Santa Maria's vertical motion history can only be explained by a gradual shift from a dominantly extrusive to a dominantly intrusive edifice growth process, resulting in isostatic uplift. In fact, ample geological evidence exists for deep magmatic intrusions contributing to volcano growth through uplift, at various timescales and different geodynamic settings (e.g. Klügel et al., 2005; Ramalho et al., 2010a,b,c; Madeira et al., 2010; Klügel et al., 2015; Ramalho et al., 2015). This process has been shown to be particularly frequent in slow-moving plates with respect to existing melting sources, as it happens with the Nubian plate (Ramalho et al., 2015). The uplift trend at Santa Maria, nevertheless, shows that intrusive processes and endogenous island edifice growth may still play a significant role on ocean island systems located on young lithosphere and at inter-plate settings such as the Azores.

CONCLUSIONS

In this study we have reconstructed, for the first time, the evolutionary history of Santa Maria Island in the Azores, with respect to the timing and magnitude of its vertical movements. Santa Maria constitutes the perfect case study to investigate the mechanisms behind ocean island uplift because the island is located in a geodynamic setting where a clear subsidence trend should be expected. However, our investigations revealed a complex evolutionary history spanning ~6 Ma, with pronounced subsidence until ~3.5 Ma, followed by an uplift trend that extended to the present. Furthermore, our study was also the first to constrain the exact time of emergence for this island, the oldest in the archipelago.

Santa Maria Island first emerged by surtseyan activity at ~6 Ma. Increased volcanism sustained the transition from emergent island stage to the subaerial shield stage, consolidating the island edifice and assuring its survival above sea level. This transition was characterized by a gradual shift from monogenetic volcanism to polygenetic shield volcanism, culminating with the formation of a broad shield volcano at around 5.8–5.3 Ma. It was also around this time that the edifice entered a pronounced subsidence trend that was to last up to ~3.5 Ma. The following stage in the evolution of the island edifice corresponds to an erosional stage characterized by topographical decay, subsidence, and marine sedimentation, with occasional low-volume submarine volcanism. This stage lasted until ~4.1 Ma, eventually leading to a partial or – more probably – almost complete truncation of the existing volcanic edifice, which at this moment resembled a wide sandy shoal punctuated by occasional residual or juvenile (surtseyan) islets. This erosional period is extremely important for palaeo- and neo-biogeographical studies as, probably, nearly all of the terrestrial species that had colonized the first island of Santa Maria must have disappeared when the island became a guyot. With renewed volcanism, the edifice eventually emerged again above sea level at about 4.1 Ma, this time essentially concentrated on the eastern side of the previous edifice. Sustained volcanic activity lasted until ~3.5 Ma, leading to considerable lateral growth by progradation of coastal lava-fed deltas, as subsidence progressed. At ~3.5 Ma, however, the island experienced a major change in its evolution, characterized by waning volcanism (lasting up to 2.8 Ma), gradual erosion, and a reversal to an uplift trend. This trend extended to the present, resulting in over 200 m of uplift and leading to the generation of a series of marine terraces on the windward side. It is precisely this uplift trend that is responsible for the exposure of superb volcanic and sedimentary marine sequences along Santa Maria's coastal cliffs, which make this island so famous amongst the Azores Archipelago.

The fact that an island located in this particular geotectonic context experienced such a pronounced uplift trend is remarkable and raises important questions concerning possible uplift mechanisms. Our analyses suggest that only one plausible uplift mechanisms may account for Santa Maria's reversal from the expected subsidence trend to a long-term uplift trend: localized uplift as a result of a shift from dominantly extrusive to dominantly intrusive edifice growth, accompanied by crustal thickening. Further research is therefore necessary to investigate the island's crustal and upper mantle in order to confirm the proposed crustal thickening.

APPENDIX

This section only applies to papers containing an appendix.

ACKNOWLEDGMENTS

This work resulted from the project "Investigation of Island Uplift of the Azores Island region" (TH1530/6-1) funded by DFG - The German Research Foundation. R. Ramalho acknowledges his FP7-PEOPLE-2011-IOF Marie Curie Fellowship. We also kindly acknowledge the following persons and institutions for all the support given during the course of this work: The Regional Government of the Azores; Drs. R. Câmara, J. Bairos, N. Moura, and J. Pombo of Serviços de Ambiente da Ilha de Santa Maria, for all the support in the field; Clube Naval de Sta Maria and particularly our skipper M. Cabral for numerous boat trips to study the island; Dra M. Antunes at Secretaria Regional do Turismo e Transportes for providing us the digital altimetric database and aerial photo coverage used in this study; our colleagues at CVARG, University of Azores, for their kind support; SATA Air Azores for facilitating the transportation of equipment and samples; finally, but not the least, all the participants of the several International Workshops "Palaeontology in Atlantic Islands" who over the years (2009–2014) participated in the fieldwork, in particular C. Rebelo, C. Melo, P. Madeira, R. Cordeiro, and R. Meireles. We also thank M. Miranda for the helpful discussion about the evolution of the Azores Triple Junction. Finally, we would like to thank D. Geist, A. Klügel, V. Acocella (reviewers), J. Colgan (U.S. Geological Survey internal reviewer), Associate Editor Luca Ferrari, and Editor Brad Singer for insightful comments that helped to improve this manuscript. Any use of trade, product, or firm names is for descriptive purposes only and does not imply endorsement by the U.S. Government.

REFERENCES CITED

Abdel-Monem, A., Fernandez, L., and Boone, G., 1975. K-Ar ages from the eastern Azores group (Santa Maria, São Miguel and the Formigas islands). Lithos v. 8, no. 4, p. 247–254.

Agostinho, J., 1931. The volcanoes of the Azores Islands. Bulletin Volcanologique v. 8, no. 1, p. 123–138.

Ali, M.Y., Watts, A.B., and Hill, I., 2003. A seismic reflection profile study of lithospheric flexure in the vicinity of the Cape Verde Islands. Journal of Geophysical Research (Solid Earth) v. 108, no. B5, p. 2239–2263.

Asimow, P.D., Dixon, J.E., and Langmuir, C.H., 2004. A hydrous melting and fractionation model for mid-ocean ridge basalts: Application to the Mid-Atlantic Ridge near the Azores. Geochemistry, Geophysics, Geosystems v. 5, no. 1, Q01E16.

Ávila, S.P., Cachão, M., Ramalho, R.S., Botelho, A.Z., Madeira, P., Rebelo, A.C., Cordeiro, R., Melo, C., Hipólito, A., Ventura, M.A., and Lipps, J.H., 2015a. The palaeontological heritage of Santa Maria Island (Azores: NE Atlantic): a re-evaluation of geosites in GeoPark Azores and their use in geotourism. Geoheritage, p. 1–17.

Ávila, S.P., Cordeiro, R., Rodrigues, A.R., Rebelo, A.C., Melo, C., Madeira, P., and Pyenson, N.D., 2015b. Fossil Mysticeti from the Pleistocene of Santa Maria Island, Azores (NE Atlantic Ocean), and the prevalence of fossil cetaceans on oceanic islands. Palaeontologia Electronica 18.2.27A: 1-12. palaeo-electronica.org/content/2015/1225-oceanic-island-fossil-cetacean.

Ávila, S.P., Madeira, P., Da Silva, C.M., Cachão, M., Landau, B., Quartau, R. and Martins, A.M., 2008. Local disappearance of bivalves in the Azores during the last glaciation. Journal of Quaternary Science, v. 23, no. 8, p. 777-785.

Ávila, S.P., Madeira, P., Zazo, C., Kroh, A., Kirby, M., da Silva, C.M., Cachão, M., Frias Martins, A.M., 2009. Palaeoecology of the Pleistocene (MIS 5.5) outcrops of Santa Maria Island (Azores) in a complex oceanic tectonic setting. Palaeogeography, Palaeoclimatology, Palaeoecology v. 274, no. 1-2, p. 18–31.

Ávila, S.P., Melo, C., Silva, L., Ramalho, R.S., Quartau, R., Hipólito, A., Cordeiro, R., Rebelo, A.C., Madeira, P., Rovere, A. and Hearty, P.J., 2015c. A review of the MIS 5e highstand deposits from Santa Maria Island (Azores, NE Atlantic): palaeobiodiversity, palaeoecology and palaeobiogeography. Quaternary Science Reviews, v. 114, p. 126-148.

Ávila, S.P., Ramalho, R.S., Habermann, J.M., Quartau, R., Kroh, A., Berning, B., Johnson, M., Kirby, M.X., Zanon, V., Titschack, J., Goss, A., Rebelo, A.C., Melo, C., Madeira, P., Cordeiro, R., Bagaço, L., Hipólito, A., Johnson, M., Uchman, A., Marques da Silva, C., Cachão, M., and Madeira, J., 2015d. Palaeoecology, taphonomy, and preservation of a lower Pliocene shell bed (coquina) from a volcanic oceanic island (Santa Maria Island, Azores). Palaeogeography, Palaeoclimatology, Palaeoecology, v. 430, p .57-73.

Ávila, S.P., Ramalho, R.S., and Titschack, J., 2016. The marine fossil record at Santa Maria Island (Azores), in Küppers, U., and Beier, C. (Eds) Volcanoes of the Azores. Active Volcanoes of the World. Springer Verlag, Berlin Heilderberg, Germany.

Ávila, S.P., Ramalho, R.S. and Vullo, R., 2012. Systematics, palaeoecology and palaeobiogeography of the Neogene fossil sharks from the Azores (Northeast Atlantic). Annales de Paléontologie, v. 98, no. 3, p. 167-189.

Beier, C., Haase, K. M., and Turner, S. P., 2012. Conditions of melting beneath the Azores. Lithos, v. 144–145, p. 1–11.

Beier, C., Mata, J., Stöckhert, F., Mattielli, N., Brandl, P.A., Madureira, P., Genske, F.S., Martins, S., Madeira, J., and Haase, K.M., 2013. Geochemical evidence for melting of carbonated peridotite on Santa Maria Island, Azores. Contributions to Mineralogy and Petrology, v. 165, no. 5, p. 823–841.

Bonatti, E., 1990. Not so hot “hot spots” in the oceanic mantle. Science, v. 250, no. 4977, p. 107–111,

Burke, K. and Wilson, J., 1972. Is the African Plate stationary? Nature, v. 239, no. 5372, p. 387–390.

Carmo, R., Madeira, J., Ferreira, T., Queiroz, G., and Hipólito, A., 2015. Volcano-tectonic structures of S. Miguel Island. In Gaspar, J.L., Guest, J.E., Duncan, A.M., Barriga, F.J.A.S. & Chester, D.K. (eds) 2015. Volcanic Geology of São Miguel Island (Azores Archipelago). Geological Society, London, Memoirs v. 44, p. 65–86.

Carmo, R., Madeira, J., Hipólito, A., and Ferreira, T., 2013. Paleoseismological evidence for historical surface rupture in S. Miguel Island (Azores). Annals of Geophysics, v. 56, no. 6, S0671.

Cas, R. and Wright, J., 1987. Volcanic Successions. Modern and Ancient: a Geological Approach to Processes, Products and Successions. Chapman & Hall, London, UK.

Catalão, J.C., Nico, G., Hanssen, R., and Catita, C., 2011. Merging GPS and atmospherically corrected InSAR data to map 3-D terrain displacement velocity. Geoscience and Remote Sensing, IEEE Transactions on v. 49, no. 6, p. 2354–2360.

Dalrymple, G.B., Alexander, E.C., Lanphere, M.A. and Kraker, G.P. 1981. Irradiation of samples for $^{40}Ar/^{39}Ar$ dating using the geological survey TRIGA reactor. In: USGS

Professional Papers. U.S. Geological Survey, Reston, VA, United States. No 1176: 29, 50 pp.

Estevens, M., and Ávila, S.P., 2007. Fossil whales from the Azores. Açoreana, v. 5, p. 140–161.

Feraud, G., Gastaud, J., Schmincke, H., Pritchard, G., Lietz, J., and Bleil, U., 1981. New K-Ar ages, chemical analyses and magnetic data of rocks from the islands of Santa Maria (Azores), Porto Santo and Madeira (Madeira Archipelago) and Gran Canaria (Canary Islands). Bulletin of Volcanology, v. 44, no. 3, p. 359–375.

Feraud, G., Kaneoka, I., and Allègre, C.J., 1980. K/Ar ages and stress pattern in the Azores: Geodynamic implications. Earth and Planetary Science Letters, v. 46, no. 2, p. 275 – 286.

Gente, P., Dyment, J., Maia, M., and Goslin, J., 2003. Interaction between the Mid-Atlantic Ridge and the Azores hotspot during the last 85 Myr: Emplacement and rifting of the hot spot-derived plateaus. Geochemistry, Geophysics, Geosystems, v. 4, no. 10, 8514.

Grigg, R., and Jones, A., 1997. Uplift caused by lithospheric flexure in the Hawaiian Archipelago as revealed by elevated coral deposit. Marine Geology, v. 141, no. 1-4, p. 11–25.

Hearty, P.J., Hollin, J.T., Neumann, A.C., O'Leary, M.J., and McCulloch, M., 2007. Global sea-level fluctuations during the last integlaciation (MIS 5e). Quaternary Science Reviews, v. 26, p. 2090-2112.

Hipólito, A., Madeira, J., Carmo, R., and Gaspar, J.L., 2013. Neotectonics of Graciosa Island (Azores): a contribution to seismic hazard assessment of a volcanic area in a complex geodynamic setting. Annals of Geophysics, v. 56, no. 6, S0677.

Huppert, K.L., Royden, L.H., and Perron, J.T., 2015. Dominant influence of volcanic loading on vertical motions of the Hawaiian Islands. Earth and Planetary Science Letters, v. 418, p. 149–171.

Janssen, A.W., Kroh, A., and Ávila, S.P., 2008. Early Pliocene heteropods and pteropods (Mollusca, Gastropoda) from Santa Maria (Azores, Portugal): systematics and biostratigraphic implications. Acta Geologica Polonica, v. 58, p. 355–369.

Johnson, C.L., Wijbrans, J.R., Constable, C.G., Gee, J., Staudigel, H., Tauxe, L., Forjaz, V.-H., and Salgueiro, M., 1998. $^{40}Ar/^{39}Ar$ ages and paleomagnetism of São Miguel lavas, Azores. Earth and Planetary Science Letters, v. 160, no. 3–4, p. 637–649.

Jones, J. and Nelson, P., 1970. The flow of basalt lava from air into water, its structural expression and stratigraphic significance. Geological Magazine, v. 107, no. 1, p. 13–19.

Kirby, M.X., Jones, D.S., and Ávila, S.P., 2007. Neogene shallow-marine paleoenvironments and preliminary Strontium isotope chronostratigraphy of Santa Maria Island, Azores. Açoreana, v. 5, p. 112–125.

Klügel, A., Hansteen, T., and Galipp, K., 2005. Magma storage and underplating beneath Cumbre Vieja volcano, La Palma (Canary Islands). Earth and Planetary Science Letters, v. 236, no. 1-2, p. 211–226.

Klügel, A., Longpré, M.-A., García-Cañada, L., and Stix, J., 2015. Deep intrusions, lateral magma transport and related uplift at ocean island volcanoes. Earth and Planetary Science Letters, v. 431, p. 140–149.

Krause, D.C. and Watkins, N.D., 1970. North Atlantic crustal genesis in the vicinity of the Azores. Geophysical Journal International, v. 19, no. 3, p. 261–283.

Kuiper, K., Deino, A., Hilgen, F., Krijgsman, W., Renne, P., and Wijbrans, J., 2008. Synchronizing rock clocks of Earth history. Science, v. 320, no. 5875, p. 500–504.

Laughton, A.S. and Whitmarsh, R.B., 1974. The Azores-Gibraltar plate boundary. In L. Kristjansson (ed.) *Geodynamics of Iceland and the North Atlantic Area*, D. Reidel Publ. Co., Dordrecht, p. 63-81.

Lee, J.-Y., Marti, K., Severinghaus, J. P., Kawamura, K., Yoo, H.-S., Lee, J. B., and Kim, J. S., 2006. A redetermination of the isotopic abundances of atmospheric Ar. Geochimica et Cosmochimica Acta, v. 70, no. 17, p. 4507–4512.

Lourenço, N., Miranda, J.M., Luís, J.F., Ribeiro, A., Victor, L. M., Madeira, J., and Needham, H., 1998. Morpho-tectonic analysis of the Azores Volcanic Plateau from a new bathymetric compilation of the area. Marine Geophysical Researches, v. 20, no. 3, p. 141–156.

Luís, J.F., and Miranda, J.M., 2008. Reevaluation of magnetic chrons in the North Atlantic between 35 N and 47 N: implications for the formation of the Azores Triple Junction and associated plateau. Journal of Geophysical Research: Solid Earth, (1978–2012) v. 113, no. B10.

Luís, J.F., Miranda, J.M., Galdeano, A., Patriat, P., Rossignol, J.C., and Mendes Victor, L.A., 1994. The Azores triple junction evolution since 10 Ma from an aeromagnetic survey of the Mid-Atlantic Ridge. Earth and Planetary Science Letters, v. 125, p. 439-459.

Madeira, J., 1986. Geologia estrutural e enquadramento geotectónico da Ilha de Santa Maria (Açores). Master's thesis, Departamento de Geologia da Faculdade de Ciências da Universidade de Lisboa.

Madeira, J., and Brum da Silveira, A., 2003. Active tectonics and first paleoseismological results in Faial, Pico and S. Jorge islands (Azores, Portugal). Annals of Geophysics, v. 46, no. 5, p. 733-761.

Madeira, J., Brum da Silveira, A., Hipólito, A., and Carmo, R., 2015. Active tectonics along the Eurasia-Nubia boundary: data from the central and eastern Azores Islands. In Gaspar, J.L., Guest, J.E., Duncan, A.M., Barriga, F.J.A.S. & Chester, D.K. (eds), Volcanic Geology of São Miguel Island (Azores Archipelago), Geological Society, London, Memoirs v. 44, p. 15–32.

Madeira, J., Mata, J., Mourão, C., Brum da Silveira, A., Martins, S., Ramalho, R.S., and Hoffmann, D., 2010. Volcano-stratigraphic and structural evolution of Brava Island (Cape Verde) from $^{40}Ar/^{39}Ar$, U/Th and field constraints. Journal of Volcanology and Geothermal Research, v. 196, no. 3-4, p. 219–235.

Madeira, J. and Ribeiro, A., 1990. Geodynamic models for the Azores triple junction: a contribution from tectonics. Tectonophysics, v. 184, no. 3, p. 405–415.

Madeira, P., Kroh, A., Cordeiro, R., Meireles, R., and Ávila, S.P., 2011. The fossil echinoids of Santa Maria Island, Azores (Northern Atlantic Ocean). Acta Geologica Polonica, v. 61, p. 243–264.

Madureira, P., Moreira, M., Mata, J., and Allégre, C. J., 2005. Primitive neon isotopes in Terceira Island (Azores archipelago). Earth and Planetary Science Letters, v. 233, no. 3, p. 429–440.

Marques, F.O., Catalão, J.C., DeMets, C., Costa, A.C.G., and Hildenbrand, A., 2013. GPS and tectonic evidence for a diffuse plate boundary at the Azores Triple Junction. Earth and Planetary Science Letters, v. 381, p. 177–187.

McNutt, M. and Menard, H. W., 1978. Lithospheric flexure and uplifted Atolls. Journal of Geophysical Research (Solid Earth), v. 83, no. B3, p. 1206–1212.

Meireles, R.P., Quartau, R., Ramalho, R.S., Rebelo, A.C., Madeira, J., Zanon, V. and Ávila, S.P., 2013. Depositional processes on oceanic island shelves–Evidence from storm-generated Neogene deposits from the mid-North Atlantic. Sedimentology, v. 60, no 7, p. 1769-1785.

Menard, H., 1983. Insular erosion, isostasy, and subsidence. Science, v. 220, no. 4600, p. 913–918.

Menendez, I., Silva, P., Martin-Betancor, M., Perez-Torrado, F., Guillou, H., and Scaillet, S., 2008. Fluvial dissection, isostatic uplift, and geomorphological evolution of volcanic islands (Gran Canaria, Canary Islands, Spain). Geomorphology, v. 102, no. 1, p. 189–203.

Métrich, N., Zanon, V., Créon, L., Hildenbrand, A., Moreira, M., and Marques, F.O., 2014. Is the 'Azores hotspot' a wetspot? insights from the geochemistry of fluid and melt inclusions in olivine of Pico basalts. Journal of Petrology, v 55, no. 2, p. 377–393.

Miller, K., Kominz, M., Browning, J., Wright, J., Mountain, G., Katz, M., Sugarman, P., Cramer, B., Christie-Blick, N., and Pekar, S., 2005. The Phanerozoic Record of Global Sea-Level Change. Science, v. 310, no. 5752, p. 1293–1298.

Min, K., Mundil, R., Renne, P.R., and Ludwig, K.R. 2000. A test for systematic errors in $^{40}Ar/^{39}Ar$ geochronology through comparison with U/Pb analysis of a 1.1-Ga rhyolite. Geochimica et Cosmochimica Acta, v. 64, no.1, p. 73-98.

Miranda, J.M., Luís, J.F. and Lourenço, N. 2016, The geophysical architecture of the Azores from magnetic data, in Küppers, U., and Beier, C. (Eds) Volcanoes of the Azores. Active Volcanoes of the World. Springer Verlag, Berlin Heilderberg, Germany.

Miranda, J.M., Luís, J.F., Lourenço, N. and Fernandes, R.M.S. 2015. The structure of the Azores Triple Junction: implications for São Miguel Island, in Gaspar, J.L., Guest, J.E., Duncan, A.M., Barriga, F.J.A.S. & Chester, D.K. (eds). Volcanic Geology of São Miguel Island (Azores Archipelago). Geological Society, London, Memoirs, 44, 1–3.

Miranda, J.M., Navarro, A., Catalão, J., and Fernandes, R.M.S., 2012. Surface displacement field at Terceira Island deduced from repeated GPS measurements. Journal of Volcanology and Geothermal Research, v. 217, p. 1–7.

Moore, J., 1970. Relationship between subsidence and volcanic load, Hawaii. Bulletin of Volcanology, v. 34, no. 2, p. 562–576.

Morgan, J., Morgan, W., and Price, E., 1995. Hotspot melting generates both hotspot volcanism and a hotspot swell. Journal of Geophysical Research (Solid Earth), v. 100, no. B5, p. 8045–8062.

Muecke, G.K., Ade-Hall, J.M., Aumento, F., MacDonald, A., and Reynolds, P.H., 1974. Deep drilling in an active geothermal area in the Azores. Nature, v. 252, p. 281–285.

O'Leary, M.J., Hearty, P.J., Thompson, W.G., Mitrovica, J.X., Raymo, M.E., Webster, J. M., 2013. Ice sheet collapse following a prolonged period of stable sea level during the last interglacial. Nature Geoscience, v. 6, no. 9, p. 796–800.

Parsons, B., Sclater, J., 1977. An analysis of the variation of ocean floor bathymetry and heat flow with age. Journal of Geophysical Research (Solid Earth), v. 82, no. 5, p. 803–827.

Porebski, S. and Gradzinski, R., 1990. Lava-fed Gilbert-type delta in the Polonez Cove Formation (Lower Oligocene), King George Island, West Antarctica. In: Colella, A. and Prior, D. (Eds.), Coarse Grained Deltas. v. 10. International Association of Sedimentologists Special Publication, p. 335–351.

Quartau, R., Hipólito, A., Romagnoli, C., Casalbore, D., Madeira, J., Tempera, F., Roque, C. and Chiocci, F.L., 2014. The morphology of insular shelves as a key for understanding the geological evolution of volcanic islands: Insights from Terceira Island (Azores), Geochemistry, Geophysics, Geosystems, v. 15, p. 1801–1826.

Quartau, R., Madeira, J., Mitchell, N.C., Tempera, F., Silva, P.F. and Brandão, F., 2015. The insular shelves of the Faial-Pico Ridge: a morphological record of its geologic evolution (Azores archipelago), Geochemistry, Geophysics, Geosystems, v. 16, p. 1401–1420.

Quartau, R., Madeira, J., Mitchell, N.C., Tempera, F., Silva, P.F. and Brandão, F., 2016, Reply to comment by Marques et al. on "The insular shelves of the Faial-Pico Ridge (Azores archipelago): A morphological record of its evolution", Geochemistry, Geophysics, Geosystems, DOI: 10.1002/2015GC006180.

Quartau, R., Tempera, F., Mitchell, N.C., Pinheiro, L.M., Duarte, H., Brito, P.O., Bates, R., and Monteiro J.H., 2012. Morphology of the Faial Island shelf (Azores): The interplay between volcanic, erosional, depositional, tectonic and mass-wasting processes, Geochemistry, Geophysics, Geosystems, v. 13, Q04012.

Quartau, R., Trenhaile, A.S., Mitchell, N.C., and Tempera, F., 2010. Development of volcanic insular shelves: Insights from observations and modelling of Faial Island in the Azores Archipelago, Marine Geology, v. 275, no 1–4, p. 66–83.

Ramalho, R.S., 2011. Building the Cape Verde Islands, 1st Edition. Springer.

Ramalho, R.S., Brum da Silveira, A., Fonseca, P.E., Madeira,J., Cosca, M., Cachão, M., Fonseca, M.M., and Prada, S.N., 2015. The emergence of volcanic oceanic islands on a slow-moving plate: The example of Madeira Island, NE Atlantic. Geochemistry, Geophysics, Geosystems, v. 16, no. 2, p. 522–537.

Ramalho, R.S., Helffrich, G., Schmidt, D. N., and Vance, D., 2010a. Tracers of uplift and subsidence in the Cape Verde Archipelago. Journal of the Geological Society [London], v. 167, no. 3, p. 519–538.

Ramalho, R.S., Helffrich, G., Cosca, M., Vance, D., Hoffmann, D., and Schmidt, D. N., 2010b. Episodic swell growth inferred from variable uplift of the Cape Verde hotspot islands. Nature Geoscience, v. 3, no. 11, p. 774–777.

Ramalho, R.S., Helffrich, G., Cosca, M., Vance, D., Hoffmann, D., Schmidt, D. N., 2010c. Vertical movements of ocean island volcanoes: Insights from a stationary plate environment. Marine Geology, v. 275, p. 84–95.

Ramalho, R.S., Quartau, R., Trenhaile, A.S., Mitchell, N.C., Woodroffe, C.D. and Ávila, S.P., 2013. Coastal evolution on volcanic oceanic islands: A complex interplay between volcanism, erosion, sedimentation, sea-level change and biogenic production. Earth-Science Reviews, v. 127, p. 140-170.

Rebelo, A.C., Rasser, M.W., Kroh, A., Johnson, M.E., Melo, C., Ramalho, R.S., Uchman, A., Zanon, V., Silva, L., Neto, A.I., Berning, B., M. Cachão, and Ávila, S.P. (2015) Rocking around a volcanic island shelf: neogene rhodolith beds from Malbusca, Santa Maria Island (Azores, NE Atlantic), submitted to Facies.

Rebelo, A.C., Rasser, M.W., Riosmena-Rodriguez, R., and Ávila, S.P., 2014, Rhodolith forming coralline algae in the Upper Miocene of Santa Maria Island (Azores, NE Atlantic): a critical evaluation. Phytotaxa, v. 190, no 1, p. 370–382.

Rusu, L., and Soares, C.G., 2012. Wave energy assessments in the Azores islands. Renewable Energy, v. 45, p. 183–196.

Saki, M., Thomas, C., Nippress, S. E., and Lessing, S., 2015. Topography of upper mantle seismic discontinuities beneath the North Atlantic: The Azores, Canary and Cape Verde plumes. Earth and Planetary Science Letters, v. 409, p. 193 – 202.

Schilling, J.-G., 1975. Azores mantle blob: Rare-earth evidence. Earth and Planetary Science Letters, v. 25, no. 2, p. 103 – 115.

Schmidt, R., and Schmincke, H.-U. 2000. Seamounts and island building. In Sigurdsson, H., Houghton, B., McNutt, S., Rymer, H., and Stix, J. (Eds.), Encyclopedia of volcanoes, p. 383–402. USA: Academic Press.

Schmidt, R. and Schmincke, H.-U., 2002. From seamount to oceanic island, Porto Santo, central East-Atlantic. International journal of earth sciences, vol. 91, no 4, p. 594–614.

Searle, R., 1980. Tectonic pattern of the Azores spreading centre and triple junction. Earth and Planetary Science Letters, v. 51, no. 2, p. 415 – 434.

Sepúlveda, P., Le Roux, J., Lara, L., Orozco, G., and Astudillo, V., 2015. Biostratigraphic evidence for dramatic Holocene uplift of Robinson Crusoe Island, Juan Fernandez Ridge, SE Pacific Ocean. Biogeosciences, v. 12, no. 6, p. 1993–2001.

Serralheiro, A., 2003. A geologia da ilha de Santa Maria, Açores. Açoreana, v. 10, no. 1, p. 141–192.

Serralheiro, A., Alves, C.A.M., Forjaz, V.H., and Rodrigues,B., 1987. Carta Vulcanológica dos Açores. Ilha de Santa Maria na escala 1/15 000 (folhas 1 e 2), Serviço Regional de Protecção Civil dos Açores, Universidade dos Açores and Centro de Vulcanologia.

Sibrant, A.L.R., Hildenbrand, A., Marques, F.O., and Costa, A.C.G., 2015a. Volcano-tectonic evolution of the Santa Maria Island (Azores): Implications for paleostress evolution at the western Eurasia–Nubia plate boundary. Journal of Volcanology and Geothermal Research, v. 291, p. 49–62.

Sibrant, A.L.R., Hildenbrand, A., Marques, F.O., Weiss, B., Boulesteix, T., Húbscher, C., Lüdmann, T., Costa, A.C.G., and Catalão, J.C., 2015b. Morpho-structural evolution of a volcanic island developed inside an active oceanic rift: S. Miguel Island (Terceira Rift, Azores). Journal of Volcanology and Geothermal Research, v. 301, p. 90–106.

Smith, J. and Wessel, P., 2000. Isostatic consequences of giant landslides on the Hawaiian Ridge. Pure and Applied Geophysics, v. 157, no. 6, p. 1097–1114.

Staudigel, H. and Schmincke, H., 1984. The Pliocene seamount series of La Palma/Canary Islands. Journal of Geophysical Research (Solid Earth), v. 89, no. B13, p. 11195–11215.

Stein, C. and Stein, S., 1992. A model for the global variation in oceanic depth and heat flow with lithospheric age. Nature, v. 359, no. 6391, p. 123–129.

Storetvedt, K.M., Serralheiro, A., Moreira, M., and Abranches, M.C., 1989. Magnetic structure and evolution of the island of Santa Maria, Azores. Physics of The Earth and Planetary Interiors, v. 58, p. 228–238.

Trota, A., 2008. Crustal deformation studies in S. Miguel and Terceira Islands (Azores). Ph.D. thesis, Universidade dos Açores.

Vogt, P., and Jung, W., 2004. The Terceira Rift as hyper-slow, hotspot-dominated oblique spreading axis: A comparison with other slow-spreading plate boundaries. Earth and Planetary Science Letters, v. 218, no. 1-2, p. 77–90.

Walcott, R., 1970. Flexure of the lithosphere at Hawaii. Tectonophysics, v. 9, no. 5, p. 435–446.

Watts, A., and ten Brink, U., 1989. Crustal structure, flexure, and subsidence history of the Hawaiian Islands. Journal of Geophysical Research (Solid Earth), v. 94, no. B8, p. 10473–10500.

Wilson, D., Peirce, C., Watts, A., Grevemeyer, I., and Krabbenhoeft, A., 2010. Uplift at lithospheric swells—I: seismic and gravity constraints on the crust and uppermost mantle structure of the Cape Verde mid-plate swell. Geophysical Journal International, v. 182, no. 2, p. 531–550.

Zbyszewski, G. and Ferreira, O. V., 1960. Carta Geológica de Portugal - Ilha de Santa Maria (Açores), na escala 1/50 000. Serviços Geológicos de Portugal.

Zhong, S., and Watts, A., 2002. Constraints on the dynamics of mantle plumes from uplift of the Hawaiian Islands. Earth and Planetary Science Letters, v. 203, no. 1, p. 105–116.

FIGURE CAPTIONS

Figure 1. (A) Map illustrating the bathymetry and geotectonic setting of Santa Maria within the Azores Triple Junction. Note that Santa Maria is located in the southeastern corner of the Azores Plateau, wedged in between the Terceira ultra-slow spreading ridge (TR), the dextral transcurrent Gloria Fault (GF, part of the Azores-Gibraltar fault system), the currently inactive East Azores Fault Zone (EAFZ), and the early incipient Princess Alice Rift (PAR). White arrows represent the approximate spreading direction of TR. Upper right inset depicts the regional setting of the Azores archipelago within the North American (NA), Eurasian (Eu) and Nubian (Nu) triple junction. (B) Bathymetry/altimetry of Santa Maria Island edifice. Note the extensive insular shelf to the north of the present-day island. Bathymetry on both subfigures extracted from the EMODNET web portal (http://portal.emodnet-bathymetry.eu); subaerial topography generated

from a 1/5,000 scale digital altimetric database provided by Secretaria Regional do Turismo e Transportes.

Figure 2. Geological map of Santa Maria Island (A) after Serralheiro et al. (1987), with a WNW–ESE cross-section (B,) and respective key for both map and section. Approximate sample locations are plotted in the map. “P^{ta}” and “M^{te}” correspond to abbreviations of “Ponta” and “Monte”, respectively. Underlying DEM generated from a 1/5,000 scale digital altimetric database provided by Secretaria Regional do Turismo e Transportes.

Figure 3. Photoset 1 of representative palaeo sea-level markers used in this study. (A) Section at Ilhéu da Vila (looking NE), showing a palaeo sea-level at ~11 m, within the Anjos volcanic succession. Note how a subaerial lava flow formed pillow structures and hyaloclastites as it entered the sea, over a beach developed on subaerial lava flows; the passage zone marks very accurately the coeval position of sea level. (B) Section exposed at Baía da Cré (looking SSE). Note that the marine sedimentary sequence of Touril (T) Complex is overlapped by a Gilbert-type west-prograding lava-fed delta belonging to the Pico Alto Volcanic Complex (PA); locally the passage zone is exposed at ~200 m (west of Cré fault) and ~130 m (east of Cré fault) in elevation. (C) Section at Ponta do Pesqueiro Alto (looking E), comprising marine sediments and submarine effusive sequences of the Touril Complex (T), overlapped by a northward-prograding lava-fed delta belonging to the Pico Alto Volcanic Complex (PA); passage zone is located at ~130 m in elevation. White vertical arrows show MIS5e wave-cut notches. (D) Section at Ponta do Norte (looking WNW), showing overlapping lava-fed deltas and intercalated marine sediments of Pico Alto Volcanic Complex; passage zone is exposed at ~110 m in elevation,

where sample SMA30 was collected. (E) Section at Pedra-que-pica/Ponta do Castelo (looking NW). Here two conformably overlapping lava-fed deltas can be seen, marking two palaeo sea-levels at ~90 m and ~55 m, where samples SMA08 and SMA09 were collected, respectively; sample SMA02 was also collected at the basal pillow lavas of the Touril Complex. (F) Section at Ponta da Malbusca (looking N), showing the vertical stacking of submarine effusive sequences and marine sediments belonging to the Touril (T) and Pico Alto Volcanic Complex (PA). The passage zone between the submarine and subaerial volcanics occurs at ~130 m in elevation, where sample SMA03 was collected.

Figure 4. Photoset 2 of representative palaeo sea-level markers used in this study. (A) Sequence at Ponta do Norte (looking S). Note the younger lava-fed delta of Pico Alto Volcanic Complex unconformably overlapping an older lava delta of the same unit, prograding to the ENE. The passage zone on the younger lava-fed delta occurs at ~110 m in elevation, but the same passage zone can be seen at ~160 m in elevation across the Ponta do Norte fault, which has a ~50 m of apparent vertical displacement. (B) Section at Ponta do Morgado/Baía do Cura (looking SSE) exhibiting a text-book example of a Gilbert-type lava-fed delta, prograding to the east, with the passage zone at ~130 m in elevation. The vertical continuity of the eastward-dipping foresets of pillow lavas and hyaloclastites from ~130 m to present sea level shows that volcanic progradation extended beyond the coeval insular shelf edge. Note also the presence of wave-cut notches at 18–20 m and 105–110 m in elevation (pointed by the black and white arrows). (C) Staircase of marine terraces at the northeastern part of the island (looking ENE); dashed lines mark the inner edge of each terrace, i.e. the position of former shorelines. (D) Pleistocene beach composed of beach conglomerates (including rounded stranded pumice) and fossiliferous

calcarenites, exposed in a trench near Ginjal. The presence of this former beach at 85–90 m attests to the position of a palaeo-shoreline at these elevations.

Figure 5. (A) Plio-Quaternary palaeo-shoreline reconstructions based on uplifted marine terrace morphology. Lines represent the inner edge of each terrace, i.e. the position of the former shore angle (solid line = visible/high confidence; dashed line = interpreted/medium confidence; dotted = interpreted/low confidence). DEM generated from a 1/5,000 scale digital altimetric database provided by Secretaria Regional do Turismo e Transportes. (B) Cross-shore profiles (p1–p6) taken along solid black lines represented in (A); the presence of marine terraces is clearly visible in these profiles (horizontal dotted lines). (C) Photo of marine terrace staircase morphology taken from point (a) in (A), looking to ENE. Note also the Cabrestantes Fm (Cab) in the foreground.

Figure 6. Isotope correlation and age spectra (for comparison) for Santa Maria's lavas. All reported ages (results) and the heights of boxes for individual heating steps (data) are shown with 2σ levels of uncertainty (except SMA07, which features data in 1σ, age results in 2σ).

Figure 6. (continued).

Figure 7. Vertical motion reconstructions for Santa Maria Island with the “tectonic correction” on relevant sea-level tracers (A) and without the “tectonic correction” (B); reference eustatic curve from Miller at al. (2005). Horizontal bars correspond to 2σ uncertainty in the age, vertical bars to the uncertainty in elevation (which reflects both the instrumental uncertainty in elevation determination and the uncertainty in the definition of a palaeo sea-level tracer). Vertical shaded

columns correspond to the approximate time intervals of each volcanic stage in the evolution of the island. The elevation of the highest marine terrace was simply defined as being 220±10 m and its age comprehended between 3.7 and 3.2 Ma, its upper and lower age bounds. Note how sea-level tracers increase in elevation with increasing age for the period 0–3.5 Ma, and conversely decrease after that. This pattern denotes an uplift trend from ~3.5–0 Ma at an approximate rate of 60 m/m.y., and a preceding subsidence trend at an approximate rate of 100 m/m.y.

Figure 8. Sketch representing the main stages in the evolutionary history of Santa Maria Island. (1a) Seamount stage, deep water substage, during the Late Miocene (?) – onset of island construction, initially as a largely-effusive submarine volcano (inferred); (1b) Seamount stage, intermediate water substage, during the Late Miocene – sustained edifice growth by vigorous submarine effusive volcanism (inferred); (2) Emergent Island stage, at ~6 Ma – first emergence above sea level by surtseyan volcanism (resulting in a precursory island) and transition to subaerial volcanism; (3) Shield-building stage, 5.7–5.3 Ma – sustained volcanism leading to the construction of a subaerial shield volcano, with accelerating subsidence; (4) Erosive stage, 5.3–4.3 Ma – waning volcanism, erosion, and subsidence, leading to the partial or, most probably, complete truncation of the existing island edifice, and extensive marine sedimentation; the edifice resembled a wide sandy shoal by the end of this stage; (5) First rejuvenated stage, 4.3–3.5 Ma – renewed vigorous volcanism builds a new island edifice off-centered to the east of the old edifice, resulting in significant eastwards and westwards coastal advancement by progradation of lava-fed deltas, under continued subsidence; coastal progradation to east overlapped existing shelf edge; (6) Second rejuvenated stage, 3.2–2.8 Ma, uplift since ~3.5 Ma – waning volcanism

and a reversal to an uplift trend resulted in topographical decay and the generation of marine terraces; sporadic low-volume monogenetic volcanism continued until 2.8 Ma, when the island's volcanic life ended; (7) Uplifted island stage, ~3.5 (or 2.8) Ma to the present – continuous uplift and erosion, with marine erosion particularly concentrated on the windward side, leading to the present-day topography, characterized by a staircase of marine terraces on the western side, and high (often plunging) coastal cliffs around the island.

Table 1. Summary of $^{40}Ar/^{39}Ar$ geochronology results of palaeo sea-level marker information used in this study. All reported ages are shown with 2σ levels of uncertainty.

[1]GSA Data Repository item 2016300, Spreadsheet containing age calculation information and raw data for CO_2-laser incremental heating $^{40}Ar/^{39}Ar$ spectra of selected samples as presented in Fig. 6, is available online at http://www.geosociety.org/pubs/ft2016.htm, or on request from editing@geosociety.org or Documents Secretary, GSA, P.O. Box 9140, Boulder, CO 80301, USA.

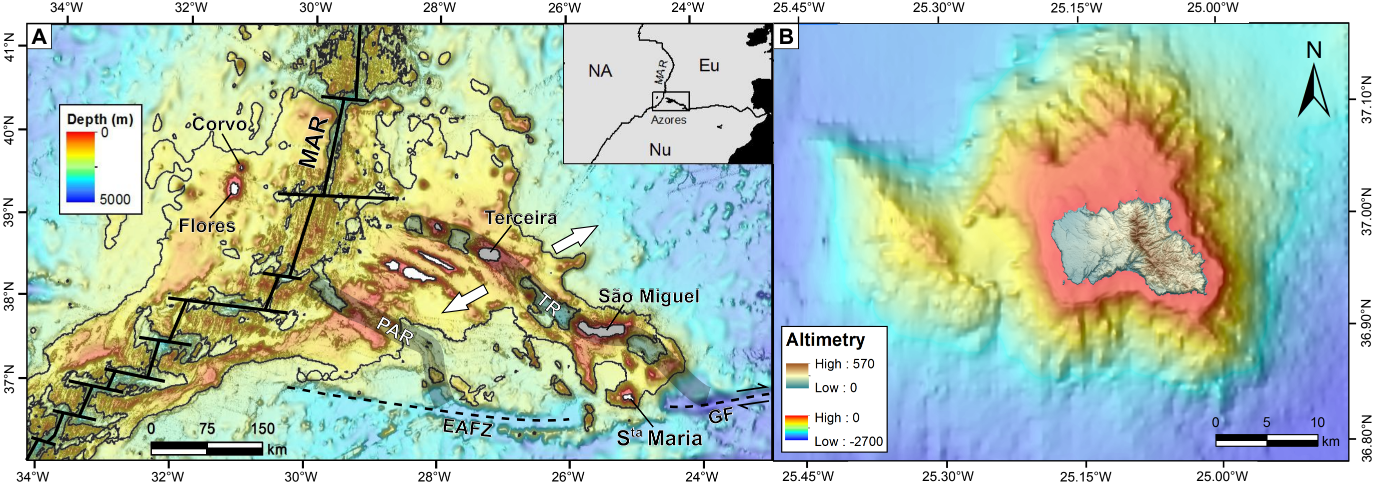
A
B
Depth (m)
0
5000
Corvo
Flores
MAR
Terceira
São Miguel
TR
PAR
EAFZ
GF
Sta Maria
NA
Eu
Nu
Azores
0 75 150 km
34°W
32°W
30°W
28°W
26°W
24°W
41°N
40°N
39°N
38°N
37°N
25.45°W
25.30°W
25.15°W
25.00°W
37.10°N
37.00°N
36.90°N
36.80°N
N
Altimetry
High : 570
Low : 0
High : 0
Low : -2700
0 5 10 km

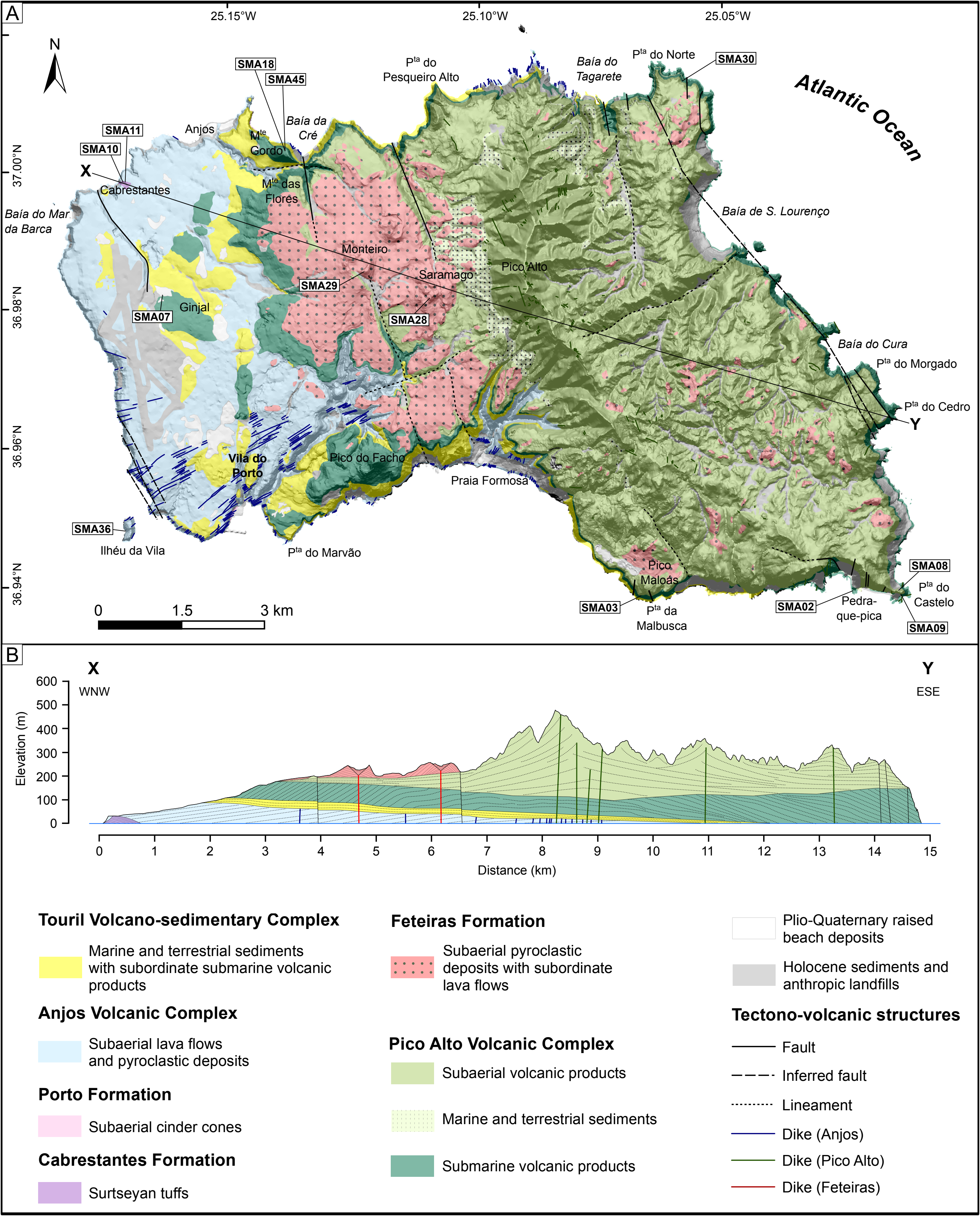
A
25.15°W
25.10°W
25.05°W
37.00°N
36.98°N
36.96°N
36.94°N
N
Atlantic Ocean
SMA18
SMA45
SMA11
SMA10
SMA29
SMA28
SMA07
SMA30
SMA36
SMA03
SMA02
SMA08
SMA09
Anjos
Mte Gordo
Baía da Cré
Mte das Flores
Cabrestantes
X
Baía do Mar da Barca
Pta do Pesqueiro Alto
Baía do Tagarete
Pta do Norte
Baía de S. Lourenço
Monteiro
Saramago
Pico Alto
Ginjal
Baía do Cura
Pta do Morgado
Pta do Cedro
Y
Vila do Porto
Pico do Facho
Praia Formosa
Ilhéu da Vila
Pta do Marvão
Pico Maloás
Pta da Malbusca
Pedra-que-pica
Pta do Castelo
0
1.5
3 km
B
X
WNW
Y
ESE
Elevation (m)
600
500
400
300
200
100
0
Distance (km)
0
1
2
3
4
5
6
7
8
9
10
11
12
13
14
15
Touril Volcano-sedimentary Complex
Marine and terrestrial sediments with subordinate submarine volcanic products
Anjos Volcanic Complex
Subaerial lava flows and pyroclastic deposits
Porto Formation
Subaerial cinder cones
Cabrestantes Formation
Surtseyan tuffs
Feteiras Formation
Subaerial pyroclastic deposits with subordinate lava flows
Pico Alto Volcanic Complex
Subaerial volcanic products
Marine and terrestrial sediments
Submarine volcanic products
Plio-Quaternary raised beach deposits
Holocene sediments and anthropic landfills
Tectono-volcanic structures
Fault
Inferred fault
Lineament
Dike (Anjos)
Dike (Pico Alto)
Dike (Feteiras)

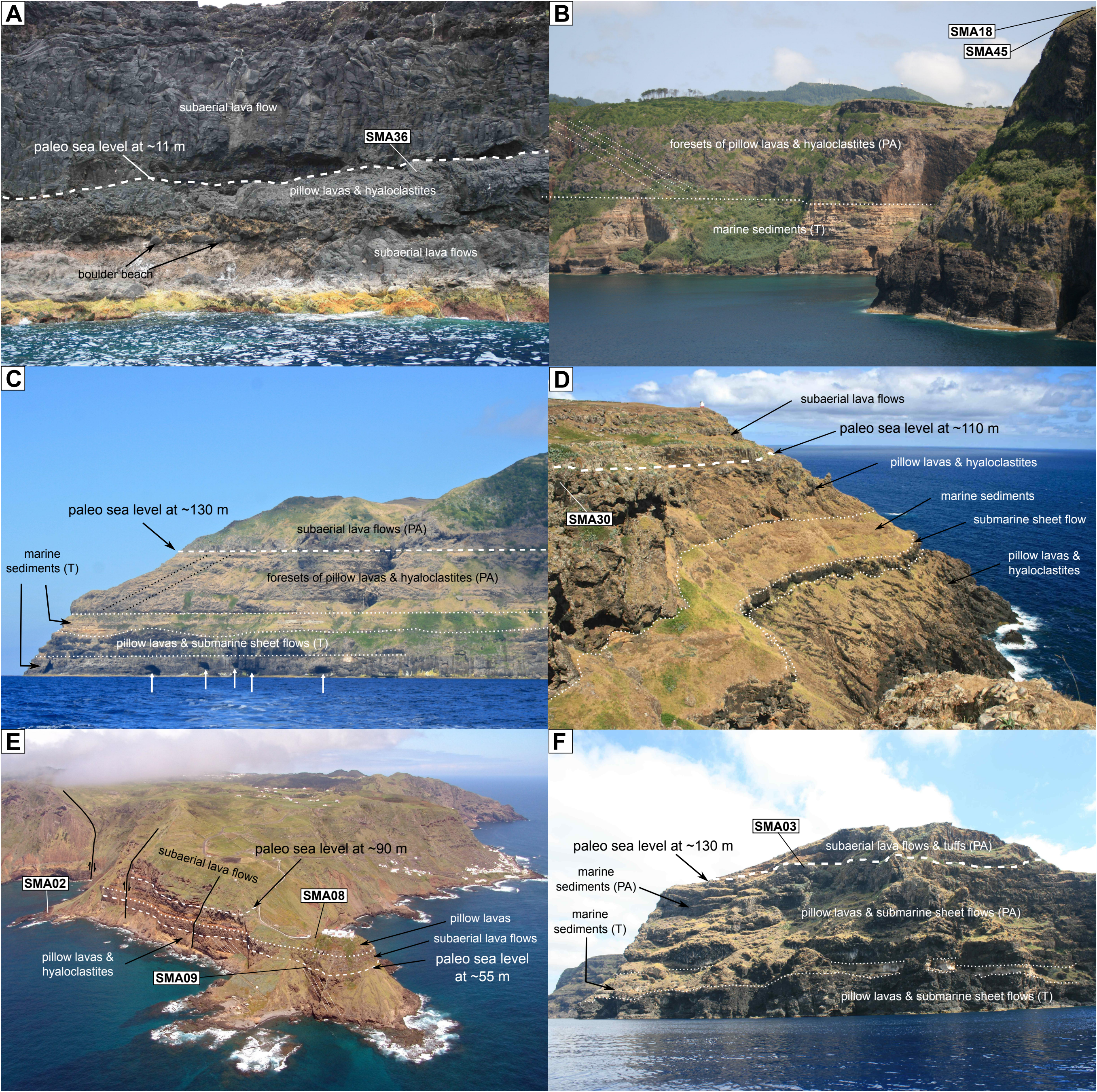
A
subaerial lava flow
paleo sea level at ~11 m
SMA36
pillow lavas & hyaloclastites
subaerial lava flows
boulder beach
B
SMA18
SMA45
foresets of pillow lavas & hyaloclastites (PA)
marine sediments (T)
C
paleo sea level at ~130 m
subaerial lava flows (PA)
marine sediments (T)
foresets of pillow lavas & hyaloclastites (PA)
pillow lavas & submarine sheet flows (T)
D
subaerial lava flows
paleo sea level at ~110 m
pillow lavas & hyaloclastites
SMA30
marine sediments
submarine sheet flow
pillow lavas & hyaloclastites
E
subaerial lava flows
paleo sea level at ~90 m
SMA02
SMA08
pillow lavas
subaerial lava flows
pillow lavas & hyaloclastites
paleo sea level at ~55 m
SMA09
F
SMA03
paleo sea level at ~130 m
subaerial lava flows & tuffs (PA)
marine sediments (PA)
marine sediments (T)
pillow lavas & submarine sheet flows (PA)
pillow lavas & submarine sheet flows (T)

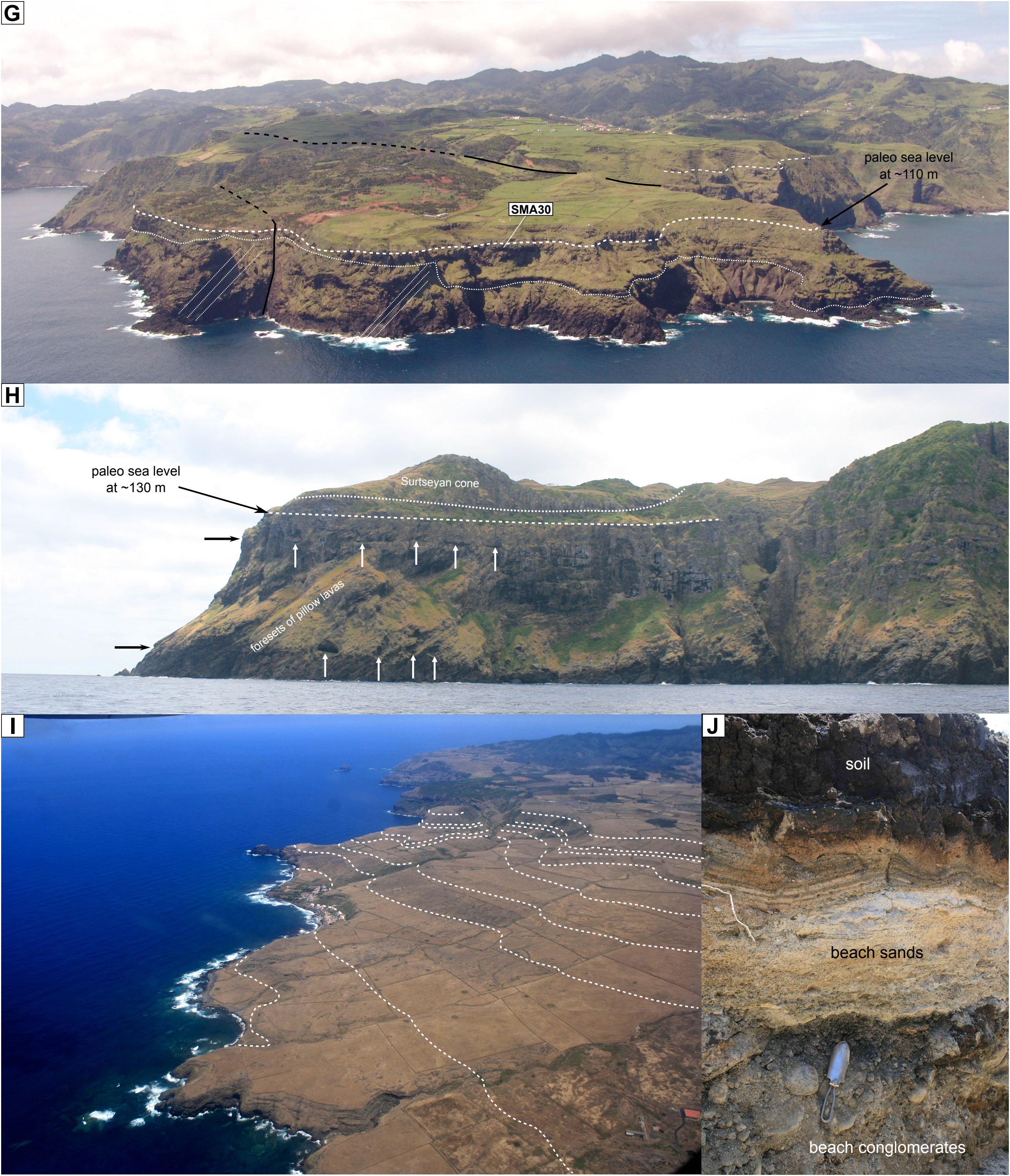
G
paleo sea level
at ~110 m
SMA30
H
paleo sea level
at ~130 m
Surtseyan cone
foresets of pillow lavas
I
J
soil
beach sands
beach conglomerates

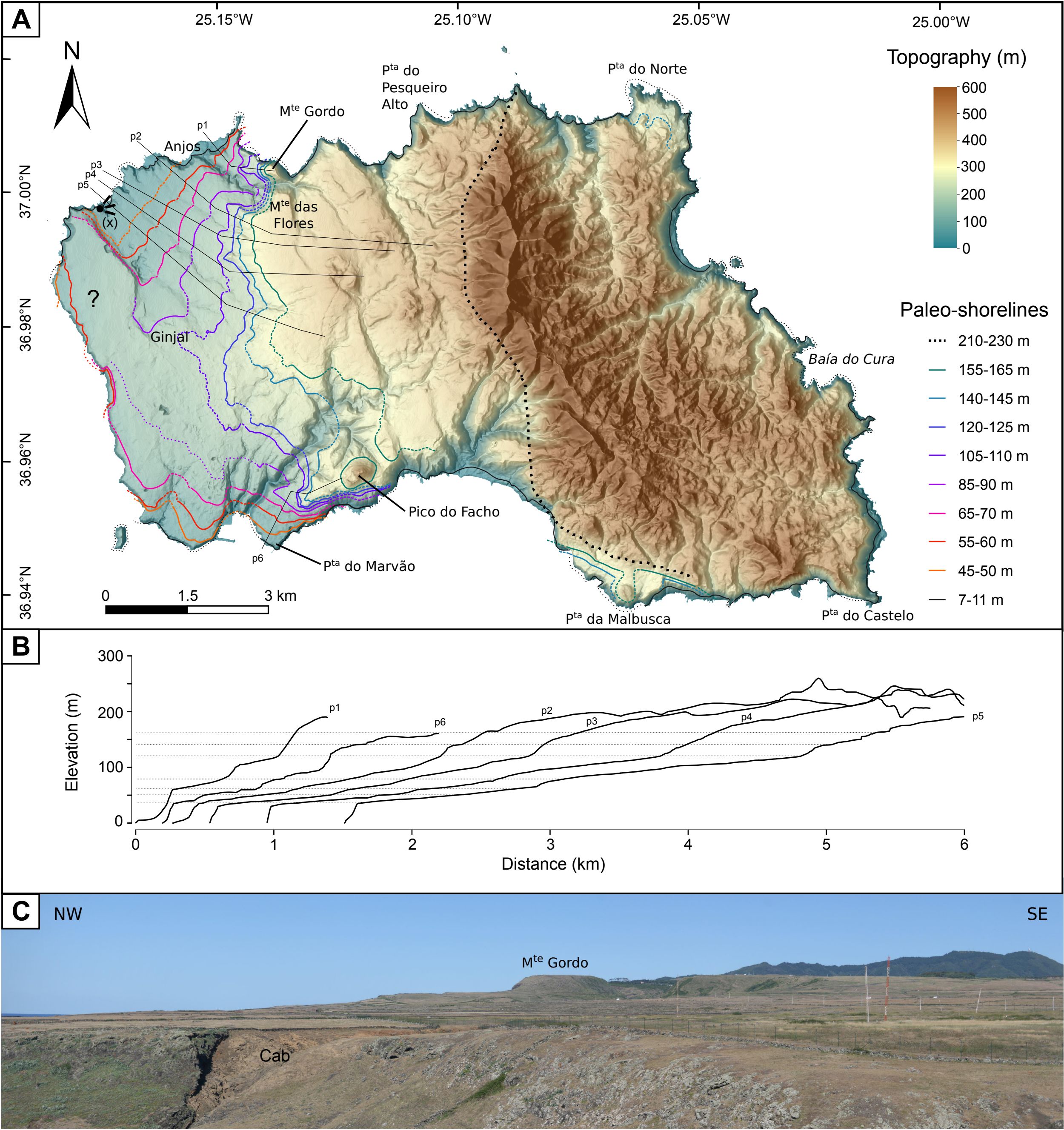
A
25.15°W
25.10°W
25.05°W
25.00°W
N
Topography (m)
600
500
400
300
200
100
0
Pta do Pesqueiro Alto
Pta do Norte
Mte Gordo
Anjos
p1
p2
p3
p4
p5
p6
37.00°N
36.98°N
36.96°N
36.94°N
Mte das Flores
(x)
?
Ginjal
Baía do Cura
Paleo-shorelines
210-230 m
155-165 m
140-145 m
120-125 m
105-110 m
85-90 m
65-70 m
55-60 m
45-50 m
7-11 m
Pico do Facho
Pta do Marvão
Pta da Malbusca
Pta do Castelo
0
1.5
3 km
B
Elevation (m)
300
200
100
0
Distance (km)
0
1
2
3
4
5
6
C
NW
SE
Mte Gordo
Cab

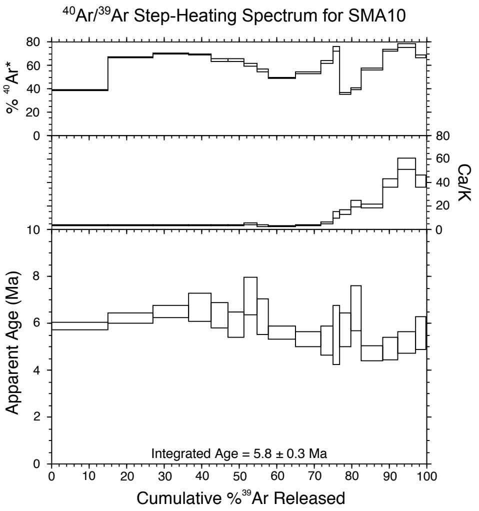
40Ar/39Ar Step-Heating Spectrum for SMA10
% 40Ar*
Ca/K
Apparent Age (Ma)
Integrated Age = 5.8 ± 0.3 Ma
Cumulative %39Ar Released

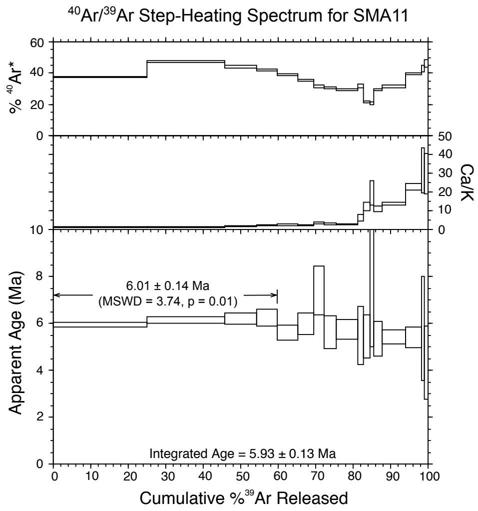
40Ar/39Ar Step-Heating Spectrum for SMA11
% 40Ar*
Ca/K
Apparent Age (Ma)
6.01 ± 0.14 Ma
(MSWD = 3.74, p = 0.01)
Integrated Age = 5.93 ± 0.13 Ma
Cumulative %39Ar Released

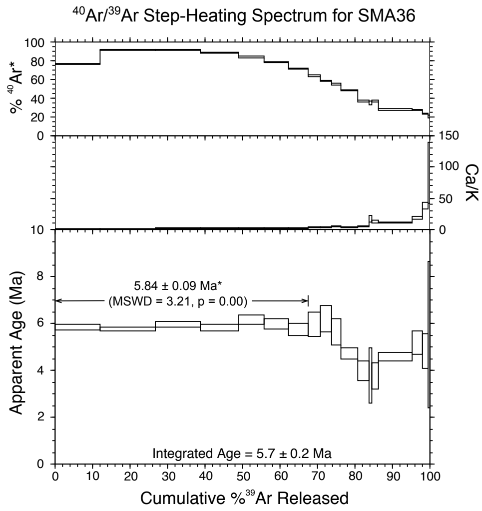
40Ar/39Ar Step-Heating Spectrum for SMA36
% 40Ar*
Ca/K
Apparent Age (Ma)
5.84 ± 0.09 Ma*
(MSWD = 3.21, p = 0.00)
Integrated Age = 5.7 ± 0.2 Ma
Cumulative %39Ar Released

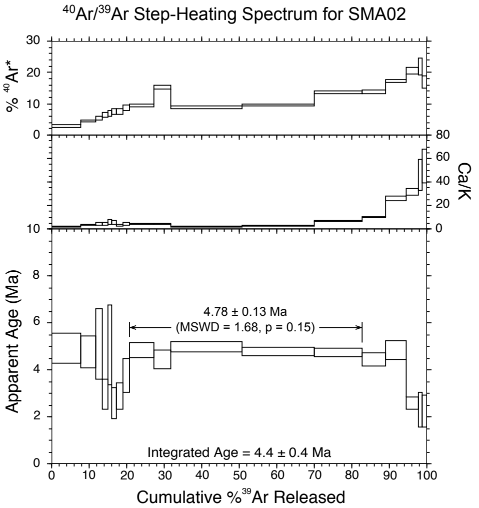
40Ar/39Ar Step-Heating Spectrum for SMA02
% 40Ar*
Ca/K
Apparent Age (Ma)
4.78 ± 0.13 Ma
(MSWD = 1.68, p = 0.15)
Integrated Age = 4.4 ± 0.4 Ma
Cumulative %39Ar Released

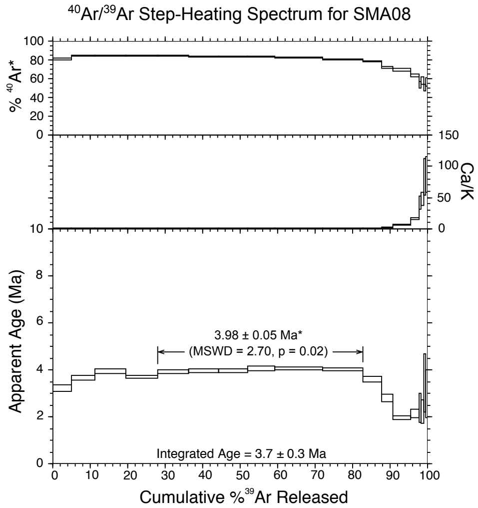
40Ar/39Ar Step-Heating Spectrum for SMA08
% 40Ar*
Ca/K
Apparent Age (Ma)
3.98 ± 0.05 Ma*
(MSWD = 2.70, p = 0.02)
Integrated Age = 3.7 ± 0.3 Ma
Cumulative %39Ar Released

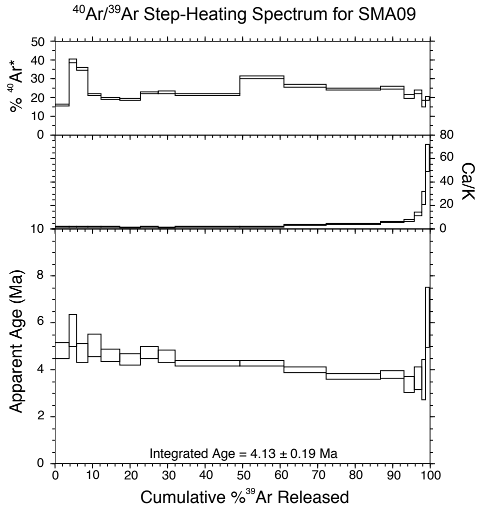
40Ar/39Ar Step-Heating Spectrum for SMA09
% 40Ar*
Ca/K
Apparent Age (Ma)
Integrated Age = 4.13 ± 0.19 Ma
Cumulative %39Ar Released

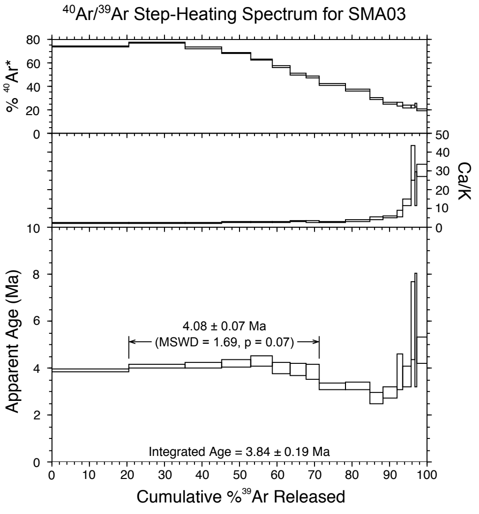
40Ar/39Ar Step-Heating Spectrum for SMA03
% 40Ar*
Ca/K
Apparent Age (Ma)
4.08 ± 0.07 Ma
(MSWD = 1.69, p = 0.07)
Integrated Age = 3.84 ± 0.19 Ma
Cumulative %39Ar Released

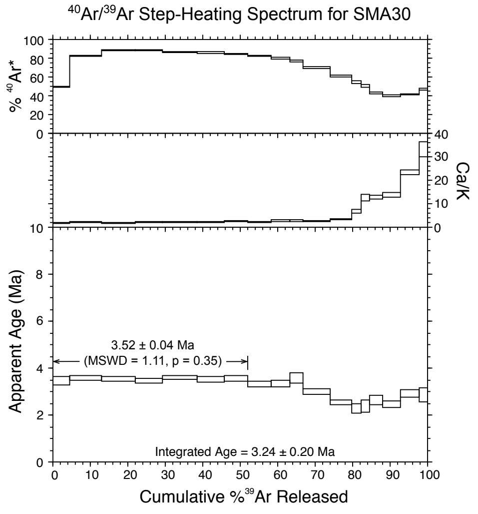
40Ar/39Ar Step-Heating Spectrum for SMA30
% 40Ar*
Ca/K
Apparent Age (Ma)
3.52 ± 0.04 Ma
(MSWD = 1.11, p = 0.35)
Integrated Age = 3.24 ± 0.20 Ma
Cumulative %39Ar Released

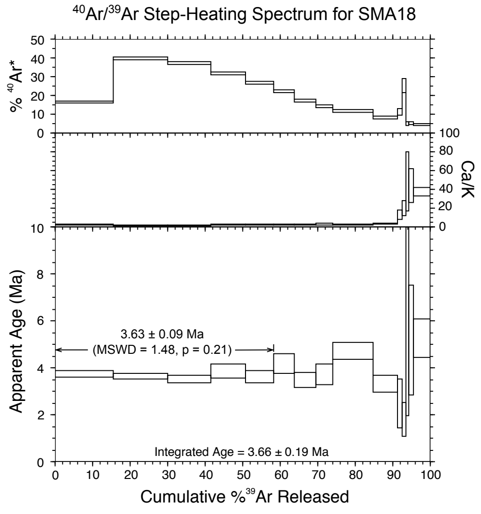
40Ar/39Ar Step-Heating Spectrum for SMA18
% 40Ar*
Ca/K
Apparent Age (Ma)
3.63 ± 0.09 Ma
(MSWD = 1.48, p = 0.21)
Integrated Age = 3.66 ± 0.19 Ma
Cumulative %39Ar Released

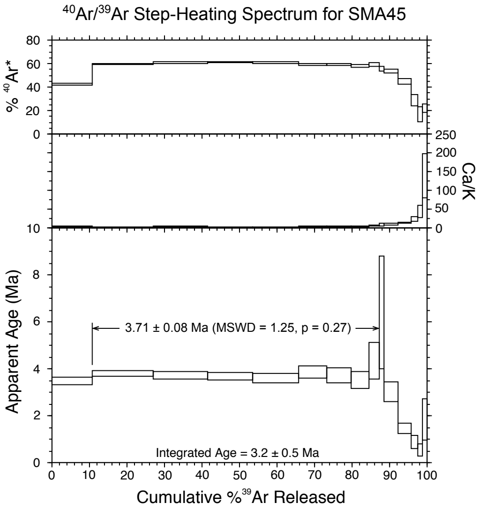
40Ar/39Ar Step-Heating Spectrum for SMA45
% 40Ar*
Ca/K
Apparent Age (Ma)
3.71 ± 0.08 Ma (MSWD = 1.25, p = 0.27)
Integrated Age = 3.2 ± 0.5 Ma
Cumulative %39Ar Released

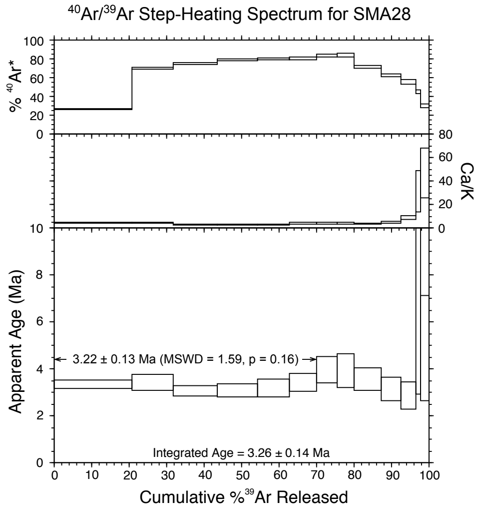
40Ar/39Ar Step-Heating Spectrum for SMA28
% 40Ar*
Ca/K
Apparent Age (Ma)
3.22 ± 0.13 Ma (MSWD = 1.59, p = 0.16)
Integrated Age = 3.26 ± 0.14 Ma
Cumulative %39Ar Released

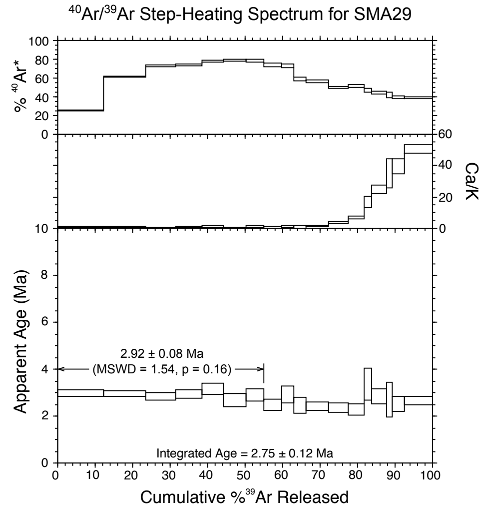
40Ar/39Ar Step-Heating Spectrum for SMA29
% 40Ar*
Ca/K
Apparent Age (Ma)
2.92 ± 0.08 Ma
(MSWD = 1.54, p = 0.16)
Integrated Age = 2.75 ± 0.12 Ma
Cumulative %39Ar Released

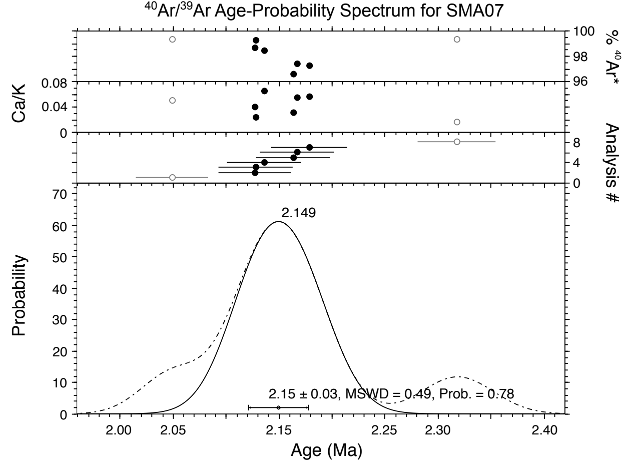

$^{40}Ar/^{39}Ar$ Age-Probability Spectrum for SMA07
% $^{40}Ar^*$
100
98
96
Ca/K
0.08
0.04
0
Analysis #
8
6
4
2
0
Probability
70
60
50
40
30
20
10
0
2.149
2.15 ± 0.03, MSWD = 0.49, Prob. = 0.78
2.00
2.05
2.15
2.25
2.30
2.40
Age (Ma)

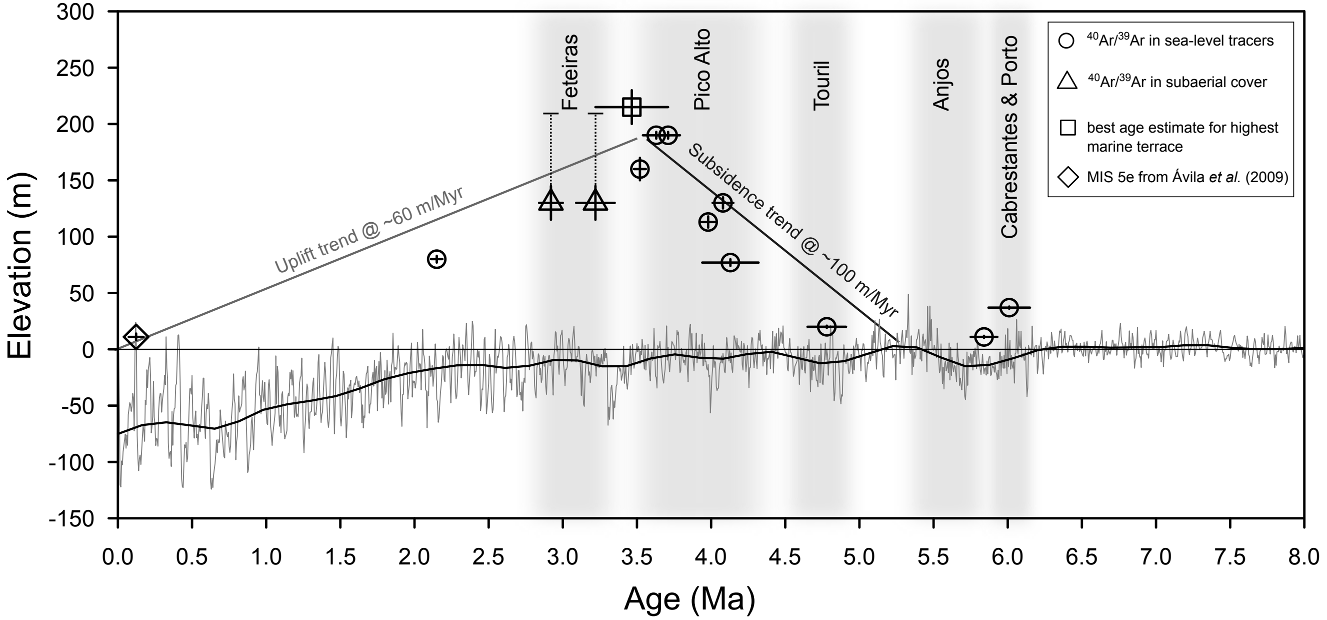

Elevation (m)
Age (Ma)
Feteiras
Pico Alto
Touril
Anjos
Cabrestantes & Porto
Uplift trend @ ~60 m/Myr
Subsidence trend @ ~100 m/Myr
40Ar/39Ar in sea-level tracers
40Ar/39Ar in subaerial cover
best age estimate for highest marine terrace
MIS 5e from Ávila et al. (2009)
300
250
200
150
100
50
0
-50
-100
-150
0.0
0.5
1.0
1.5
2.0
2.5
3.0
3.5
4.0
4.5
5.0
5.5
6.0
6.5
7.0
7.5
8.0

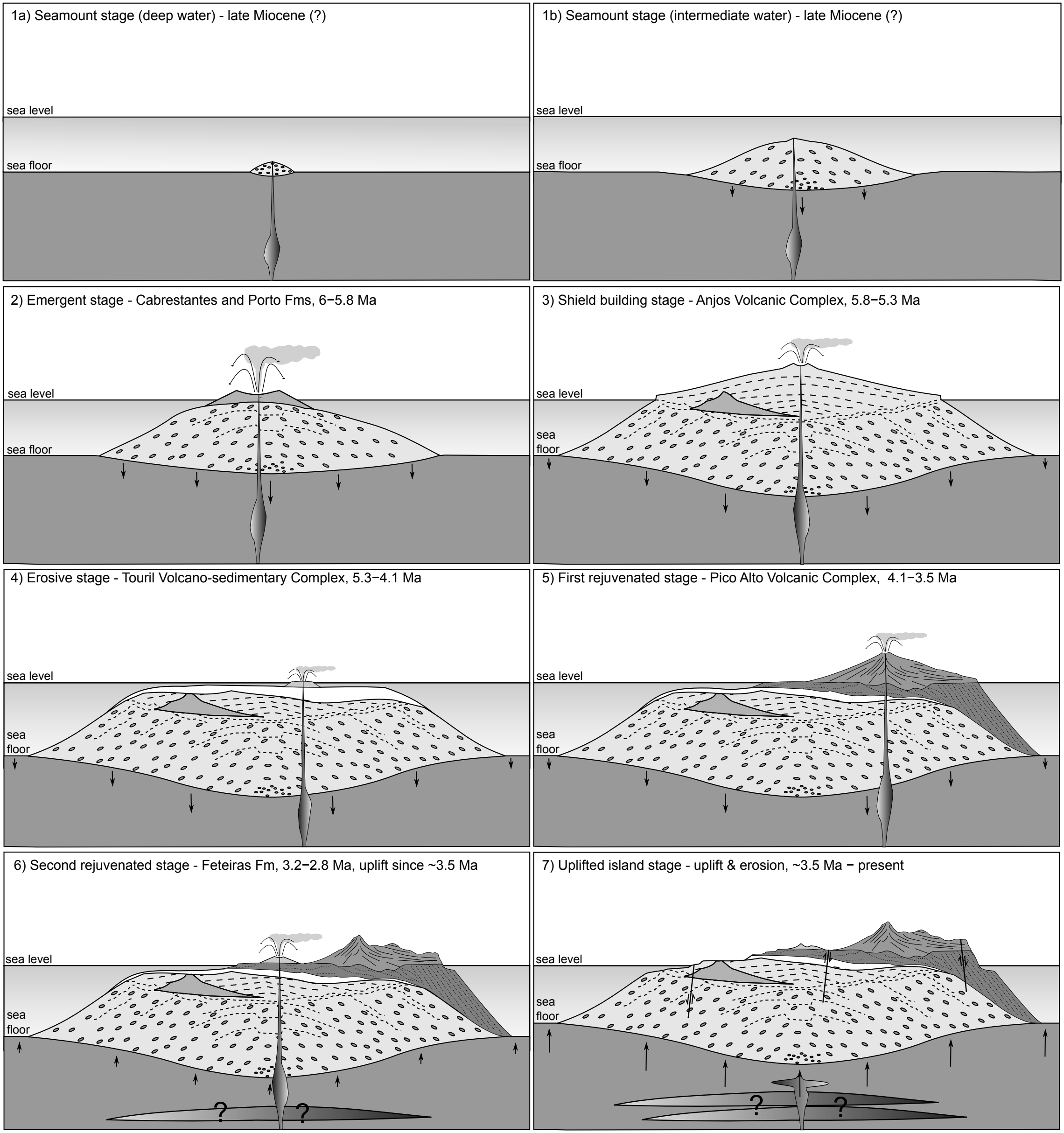
1a) Seamount stage (deep water) - late Miocene (?)
sea level
sea floor
1b) Seamount stage (intermediate water) - late Miocene (?)
sea level
sea floor
2) Emergent stage - Cabrestantes and Porto Fms, 6−5.8 Ma
sea level
sea floor
3) Shield building stage - Anjos Volcanic Complex, 5.8−5.3 Ma
sea level
sea floor
4) Erosive stage - Touril Volcano-sedimentary Complex, 5.3−4.1 Ma
sea level
sea floor
5) First rejuvenated stage - Pico Alto Volcanic Complex, 4.1−3.5 Ma
sea level
sea floor
6) Second rejuvenated stage - Feteiras Fm, 3.2−2.8 Ma, uplift since ~3.5 Ma
sea level
sea floor
?
?
7) Uplifted island stage - uplift & erosion, ~3.5 Ma − present
sea level
sea floor
?
?

Table 1. Summary of $^{40}Ar/^{39}Ar$ geochronology results of palaeo sea-level marker information used in this study. All reported ages are shown with 2σ levels of uncertainty.

Stratigraphic unit	**Sample ref.**	**Location**	**Coordinates (WGS84)**	**Elevation of palaeo-sea level marker (m)**	**Tectonic correction**	**Age (Ma±2σ)**
Cabrestantes	SMA10	Cabrestantes	N36.99828° W2517193°	37	-	5.80±0.3
	SMA11	Cabrestantes	N36.99835° W25.17199°	37	-	6.01±0.14
Anjos	SMA36	Ilhéu da Vila	N36.94187° W25.17270°	11	-	5.84±0.09
Touril	SMA02	Pedra-que-pica	N36.93011° W25.02569°	8	12	4.78±0.13
Pico Alto	SMA08	Ponta do Castelo	N36.92981° W25.01639°	91	12	3.98±0.05
Pico Alto	SMA09	Ponta do Castelo	N36.92947° W25.01673°	55	12	4.13±0.19
Pico Alto	SMA03	Ponta da Malbusca	N36.93017° W25.06856°	130	-	4.08±0.07
Pico Alto	SMA30	Ponta do Norte	N37.01257° W25.05641°	110	50	3.52±0.04
Pico Alto	SMA18	Monte Gordo	N37.00349° W25.13888°	190	-	3.63±0.09
Pico Alto	SMA45	Monte Gordo	N37.00344° W25.13876°	190	-	3.71±0.08
Feteiras	SMA28	Saramago	N36.97879° W25.11020°	215 and 130*	-	3.22±0.13
Feteiras	SMA29	Monteiro	N36.98254° W25.12535°	215 and 130*	-	2.92±0.08
Plio-Quaternary sediments	SMA07	Ginjal	N36.97928° W25.16365°	85	-	2.15±0.03

* the cones of Feteiras lie over the 210-230 m marine terrace but their subaerial products reach down to 130 m; these cones therefore provide a lower age bound for the 210-230 m palaeo-shoreline (here indicated with the medium elevation of 215 m) and an upper age bound for the 130 m palaeo-shoreline.